8 Computed Tomographic Cardiovascular Imaging

Matthew J. Budoff

Cardiac computed tomography (CT) is a robust technology for the noninvasive assessment of a spectrum of cardiovascular disease processes. This image modality has been used to provide assessment of atherosclerotic plaque burden and coronary artery disease risk through coronary calcium scoring. Although the technology has been clinically available for 20 years,[1] cardiologists and even radiologists are largely unaware of its capabilities. This chapter reviews the current clinical uses and describes some of the potential for even greater utility in the near future. Advances in spatial and temporal resolution, electrocardiographic triggering methodology, and image reconstruction software have helped in the evaluation of coronary artery anatomy and vessel patency, providing the ability to noninvasively diagnose or rule out significant epicardial coronary artery disease. Cardiac CT allows the three-dimensional (3D) simultaneous imaging of additional cardiac structures including coronary veins, pulmonary veins, atria, ventricles, aorta, and thoracic arterial and venous structures, with definition of their spatial relationships for the comprehensive assessment of a variety of cardiovascular disease processes. This chapter discusses the role of cardiac CT in the assessment of cardiovascular pathology, with an emphasis on the detection of coronary atherosclerosis.

Tomographic Imaging Modalities

Electron Beam Computed Tomography

The tomographic imaging modalities, including electron beam CT (EBCT), multidetector CT (MDCT), and magnetic resonance imaging (MRI), have advantages and limitations in the evaluation of cardiovascular disease, depending on the particular clinical questions posed. Electron beam CT is a fourth-generation CT imaging modality that is able to rapidly obtain thin tomographic cardiac slices for the evaluation of coronary artery anatomy. The speed of image acquisition is possible due to the fact that the x-ray source is stationary. In basic terms, instead of rotating the x-ray tube around the patient as conventional scanners do, the EBCT scanner has the patient positioned inside the x-ray tube, obviating the need to move any part of the scanner during image acquisition. The electron beam is emitted from the cathode, which is several feet superior to the patient's head, and then passes through a magnetic coil, which bends the beam so that it will strike one of four tungsten anode targets. The magnetic coil also steers the beam through an arc of 210 degrees. The x-ray generated from the powerful electron stream striking the tungsten anode target passes through the patient in a fan-shaped beam and strikes the detector array positioned opposite the four anodes.

Three imaging protocols are used with the electron beam CT scanner. They provide the format to evaluate anatomy, cardiovascular function, and blood flow. The imaging protocol used to study cardiovascular anatomy is called the volume scanning mode and is similar to the scanning protocol employed by conventional CT scanners. Single scans are obtained, and then the scanner couch is incremented a preset distance, usually the width of the scan slice, so that there is no overlap of anatomy. This scanning mode is utilized with and without contrast enhancement and provides high spatial resolution of cardiovascular anatomy. This technique is ideal for evaluation of the aorta, coronary arteries, and congenital heart disease. The thinnest slice available is 1.5 mm, which is not as thin as now available on multidetector scans (which have slice thickness as thin as 0.5 mm by one vendor, and 0.625 to 0.75 by most others).

The cine scanning protocol acquires images in 50 ms. Each scan is separated by an 8-ms delay, which translates to a scanning rate of 17 scans/second per target. Scanning on multiple targets simultaneously allows for large volumes of the heart to be covered with each heartbeat. Scans are acquired for the duration of the cardiac cycle. Depending on

the heart rate, up to 8 cm of the heart can be imaged in a single heartbeat. The images acquired can be displayed in a cine loop (literally a movie demonstrating motion of the heart), making assessment of wall motion, segmental thickening, and valve motion possible. Blood pool contrast enhancement is achieved by injection of contrast medium boluses via a superficial peripheral vein. The bolus amount for each image acquisition period averages 30 mL. The flow mode imaging protocol acquires a single image gated to the electrocardiogram at a predetermined point in the cardiac cycle [e.g., end-diastole (peak of the R-wave)]. Images can be obtained for every cardiac cycle or multiples thereof. Scanning is initiated before the arrival of a contrast bolus at an area of interest (e.g., left ventricular [LV] myocardium) and is continued until the contrast has washed in and out of the area. Time density curves from the region of interest can be created for quantitative analysis of flow, useful for shunt fraction determinations, as well as timing of boluses for imaging of coronary anatomy in the volume (high resolution) mode.

The ability to rapidly acquire images decreases respiratory and cardiac motion artifacts, making the modality well-suited for the evaluation of the coronary vasculature. The entire cardiac structure is imaged during a single approximate 15- to 30-second breath-hold. Electron beam CT acquires high-resolution images of the heart with temporal resolution of 50 or 100 milliseconds (ms) and prospective gating to the cardiac cycle. This allows imaging during the diastolic phase, when cardiac motion is minimized.[2] The newest generation of EBCT scanner is the e-speed scanner (GE Medical Systems, San Francisco, CA), which allow for 50-ms image acquisition in both the high-resolution and low-resolution modes, and imaging more than one level simultaneously. The faster image acquisition and multiple level imaging associated with this device further decreases breath-hold time, radiation exposure, and motion artifacts. Prospective gating (identifying the R wave and triggering at a fixed time thereafter to catch early diastole) allows for imaging of patients with a spectrum of heart rates and rhythms (including premature beats and atrial fibrillation).

Multidetector Computed Tomography

Multidetector CT (MDCT) systems were initially capable of acquiring four levels simultaneously in 2000,[3] now can obtain up to 64 levels of the heart simultaneously with ECG gating in either a prospective or retrospective mode. The MDCT differs from single-slice helical or spiral CT systems principally by the design of the detector arrays and data acquisition systems that allow the detector arrays to be configured electronically to acquire multiple levels of various slice thickness simultaneously. Thus, in the current 16-channel MDCT systems 16 slices can be acquired at nominally 0.75-mm slice widths for cardiac imaging. In MDCT systems, like the preceding generation of single-slice helical scanners, the x-ray photons are generated within a specialized x-ray tube mounted on a rotating gantry. Subsecond MDCT scanners use a rapidly rotating x-ray tube and several rows of detectors, also rotating. The tube and detectors are fitted with slip rings that allow them to continuously move through multiple 360-degree rotations. With gantry continuously rotating, the table moves the patient through the imaging plane at a predetermined speed. The relative speed of the gantry rotation table motion is the scan pitch. The smooth rapid table motion or pitch in helical scanning allows complete coverage of the cardiac anatomy in 15 to 25 seconds. A major advantage over EBCT is the improved spatial resolution and contrast resolution, allowing for a more detailed look at the coronary anatomy.[4]

Advances in MDCT technology have led to scanners that can obtain images with a scan rotation of 333 ms, and with partial scanning, image acquisition between 175 and 250 ms. Furthermore, utilizing portions of each of the images, and adding data from consecutive detectors, allows for further reduction in temporal resolution. Although it is not always possible, given the heart rate and regularity of the rhythm, most vendors are now quoting scan times approaching 110 to 140 ms using this technique (Fig. 8.1).

Multidetector CT also possesses greater versatility for peripheral vascular imaging, as the gantry opening allows the patient to be inserted from head to foot without repositioning. This is in contrast to EBCT, where the cone beam limits patient motion, where many peripheral studies need to be done in two phases (iliac to popliteal, and then the patient is rotated feet first to image popliteal to foot). The smooth rapid table motion or pitch in helical scanning allows complete coverage of the cardiac anatomy in 15 to 25 seconds. Use of the 64-slice scanner decreases this imaging window to 5 to 12 seconds for cardiac and peripheral imaging.

With MDCT, the limited temporal resolution is due to the design. The mechanical detector head has to rotate around the patient. Present versions complete a 360-degree rotation in about four-tenths of a second. These scanners' exposure times can be decreased to as little as 175 ms by utilizing only a portion of the 360-degree rotation. Approximately 210 degrees of rotation is necessary for one image, so the rotation speed can be multiplied by 0.6 to calculate image acquisition times. For example, a rotation speed of 400 ms for a 360-degree image will have a total temporal resolution

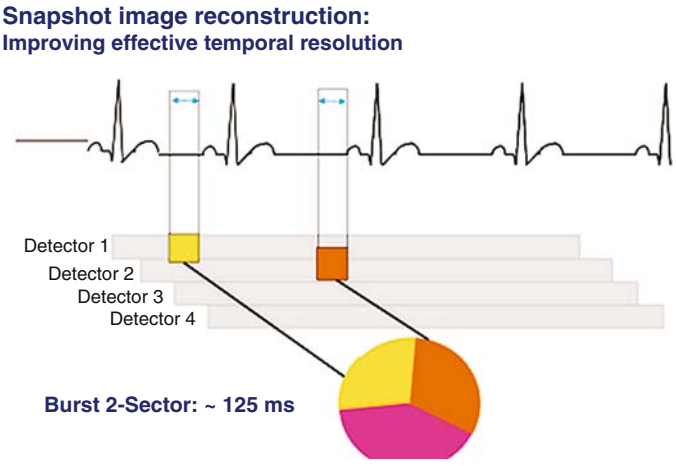

FIGURE 8.1. "Burst" technology allowing parts of each image to be used for reconstruction. In this example, portions of two consecutive images were used to allow the temporal resolution of multidetector computed tomography (MDCT) to be reduced from 265 ms to about 132 ms.

of approximately 240 ms. The manufacturers often quote 50% of the rotation speed (i.e., 200-ms image acquisition), but this only refers to the central point on the scan, and not the entire image, so this is most often somewhat misleading to the clinician or user. Simultaneous imaging from multiple detectors (now up to 64) during gantry rotation provides greater spatial resolution than EBCT (specifically thinner slices through the heart), but at the expense of temporal resolution (time to image an individual level, presenting more motion artifacts when heart rates are above 60 beats per minute).[4] Newer EBCT systems quote 9 to 11 line-pairs/cm, while MDCT has improved spatial resolution, with 14 to 16 line-pairs/cm of resolution. Although EBCT suffers from decreased signal to noise and gantry design, a disadvantage of MDCT cardiac scanning is an increase in motion artifacts and radiation exposure.[5] For cardiac imaging, there is a narrower window of acceptable heart rates for scanning with MDCT compared to EBCT, with many patients requiring pharmacologic decreases in heart rate to less than 60 beats/minute to extend diastole to the point of minimizing cardiac motion (see Multidetector Computed Tomography Angiography, below). A major current disadvantage of MDCT in cardiac scanning is an increase in radiation dose (see below).[6]

In the near term, the development and introduction of MDCT systems with increased detectors is likely. In 2005, most vendors offer a 64-row system, and the additional detector rows help to improve temporal resolution, reduce breath-hold time, and reduce contrast dose. We will observe continued rapid advancement in CT for coronary and peripheral angiography and a series of comparative studies evaluating these new CT techniques with existing measures of coronary heart disease.

Comparison of Computed Tomography to Magnetic Resonance Imaging

The strength of magnetic resonance cardiovascular imaging includes greater definition of tissue characteristics, perfusion, valvular function, lack of x-ray radiation, and lack of need for potentially nephrotoxic contrast media, compared to CT technologies. Several studies have been reported comparing this modality to coronary angiography.[7–9] Limited temporal and spatial resolution,[10] partial volume artifacts,[11] reliance on multiple breath holds, and poor visualization of the left main coronary artery[12] all reduce the clinical applicability of MR angiography. Computed tomography angiography offers advantages over MR angiography, including single breath hold to reduce respiratory motion, higher spatial resolution, reduced slice thickness, and overall study time of 35 to 50 seconds with CT techniques as compared to 45 to 90 minutes for MR angiography.[4,13] Reported sensitivities for MR angiography range from 0% to 90%.[4,7,13] Magnetic resonance angiography remains a technically challenging technique with certain limitations hindering its clinical use. The rapidity and ease with which CT coronary angiography can be performed suggest possible cost advantages compared with MR angiography and selective coronary angiography.[14]

In comparison, the strengths of CT include superior imaging of coronary arteries, higher spatial and temporal resolution, ability to scan patients with implantable metallic devices such as pacemakers and defibrillators, and shorter study times.[4]

Noncontrast Computed Tomography Imaging

Coronary Artery Calcium

Coronary artery calcium (CAC) is closely associated with coronary atheromatous plaque. Arterial calcium deposition occurs in association with atherosclerotic plaque evolution and is regulated by cellular calcification-regulating proteins.[15] A direct relationship has been established between coronary artery calcium as measured by EBCT and both histopathologic[16,17] and in vivo intravascular ultrasound[18,19] studies, which confirm the close correlation between atherosclerotic plaque burden and extent of CAC.

Electron beam CT can accurately and noninvasively quantitate CAC, and several measurements have been used.[20] Most centers and research studies have reported a calcium score measurement (Agatston method)[1] that takes into account the density and area of the calcification. The score is calculated by multiplying the lesion area by a density factor derived from the maximal Hounsfield unit (HU) within this area. The density factor was assigned in the following manner: 1 for lesions whose maximal density was 130 to 199 Hu, 2 for 200 to 299 Hu, 3 for 300 to 399 Hu, and 4 for >400 Hu. A total calcium score is determined by summing individual lesion scores from each of four anatomic sites (left main, left anterior descending, circumflex, and right coronary arteries) (Fig. 8.2). The other measures are volume

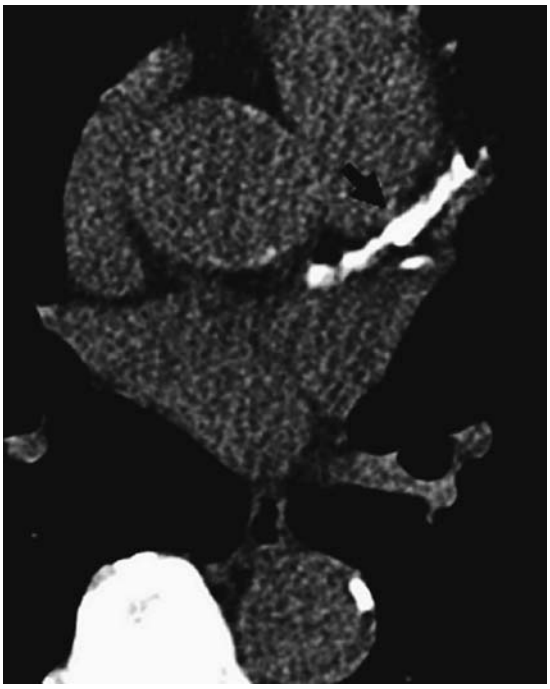

FIGURE 8.2. A computed tomography (CT) study (axial image) demonstrating calcification of the left main and left anterior descending coronary arteries. The total coronary calcium score was over 1000. Arrow, left anterior descending coronary artery calcification.

measurement and mass score. A large criticism directed at the Agatston method is increased variability (decreased reproducibility) due to image noise (a peak HU of 199 would multiply the area by a factor of 1; if that increased to 201 on a subsequent scan, it would increase the score twofold, as the density factor would be two). These small changes in measurement can double the interscan variability, leading to other measures to be proposed to allow for more accurate and reproducible measurement of CAC. The volume method of Callister et al.[21] somewhat resolves the issues of density measures, slice thickness, and spacing by computing a volume above threshold. This has been shown to be more reproducible, but fewer data are available on the prognostic values of such scores. A mass score has been introduced, but absolutely no prognostic information is available, and this requires a phantom to make this measure, which has been shown to increase image noise (which worsens reproducibility on individual scans).[22] Further research using either volume or mass scores will be needed to allow accurate clinical guidelines to be written.

Data regarding calcium score distribution in large numbers of asymptomatic persons have been published.[23] These tables can be used to classify patients on the basis of the extent of their atherosclerotic disease compared with the expected norm. In men, there is a rapid increase in the prevalence and extent of coronary calcification after age 45. Compared to men, this increase is delayed for 10 to 15 years in women.

Reproducibility of Coronary Calcium Assessment

The reproducibility of the CAC measurement is essential to utilizing this modality for assessment of the efficacy of therapeutic interventions. Reproducibility was initially a concern for repeated testing, but hardware and software improvements have reduced interscan variability to a median of 4% to 8%.[24] In addressing reproducibility issues with coronary calcium, it was noted that the most commonly used trigger time in early studies (80% of the R-R interval) is suboptimal due to increased coronary motion during atrial kick (atrial systole causing the right coronary and circumflex arteries to move rapidly). This has become particularly important with the increased use of CT for measurement of progression of atherosclerosis as well as CT coronary angiography (to improve visualization of the coronary arteries without motion artifacts). Recent studies suggest that a triggering should be initiated early in diastole rather than near the end (80%) as has been done in the past with some scanners.[2] The ideal trigger is, by definition, that which gives the least cardiac motion, and has been extensively studied for EBCT, and found to be at the end of systole (late systole or early diastole). Studies with MDCT usually conclude that 40% to 50% of the R-R interval (early diastole) is the optimal trigger for visualization of lumina with least coronary motion. Early diastolic triggering has reduced the variability of CAC to 11% to 15%.[25] With excellent inter- and intraobserver variability (1%), this test can measure plaque burden changes over time. Multidetector CT reproducibility is currently higher, although newer scanners (with 16, 32, or 64 detectors) should help in reducing this measurement error. A study of 537 patients undergoing two studies on four-slice MDCT with cardiac gating demonstrated a mean variability of 36% for volume scoring and 43% for Agatston scoring.[26]

Calcium Progression

Much interest has been directed at using CAC to measure plaque burden, and then remeasuring at some point in time to assess for progression of disease. Callister et al.[21] was one of the first studies to demonstrate a relationship between cholesterol control and atherosclerosis progression. There was a significant net increase in mean calcium-volume score among individuals not treated with cholesterol-reducing medications (mean change: 52 ± 36%, $p < .001$). There was a graded response depending upon the low-density lipoprotein (LDL) reduction with statin therapy, with those treated to LDL < 120 mg/dL demonstrating an average diminution of coronary calcium (–7% ± 23%), and those individuals treated less aggressively (LDL > 120 mg/dL) showed a calcium-volume score increase of 25% ± 22% ($p < .001$ for comparison with aggressively treated subjects).

Another study evaluated 299 patients who underwent two consecutive scans at least 12 months apart.[27] The average change in the calcium score (Agatston method) for the entire group was 33.2% ± 9.2% per year. Those patients reporting use of a statin had an annual rate of progression of 15%, compared with 39% annual increase in EBCT score for nonstatin users.

Prospective studies demonstrating a link between CAC progression and coronary events have recently been reported. The first study demonstrated, in 817 persons, that EBCT-measured progression was the strongest predictor of cardiac events.[28] This observational study suggests that continued accumulation of CAC in asymptomatic individuals is associated with increased risk of myocardial infarction (MI) in asymptomatic individuals. A second study measured the change in CAC in 495 asymptomatic subjects submitted to sequential EBCT scanning.[29] Statins were started after the initial EBCT scan. On average, MI subjects demonstrated a CAC change of 42% ± 23% yearly; event-free subjects showed a 17% ± 25% yearly change ($p = .0001$). Relative risk of having an MI in the presence of CAC progression was 17.2-fold [95% confidence interval (CI): 4.1 to 71.2] higher than without CAC progression ($p < .0001$). In a Cox proportional hazard model, the follow-up score ($p = .034$) as well as a score change >15% per year ($p < .001$) were independent predictors of time to MI. The Multi-Ethnic Study of Atherosclerosis will measure baseline CAC scores and repeat this measurement after 3.5 years in 6600 patients. Interim events, within the 3.5 years, will be measured. Future events in the subsequent 3.5 years (total 7 years follow-up) will be measured.

Coronary Artery Calcium and Obstructive Disease

In contradistinction to other noninvasive modalities that focus on diagnosis of obstructive coronary artery disease (CAD), EBCT coronary calcium represents an anatomic measure of plaque burden.[30] Studies comparing pathologic and EBCT findings have shown that the degree of luminal narrowing is weakly correlated with the amount of calcification on a segment-by-segment basis,[31] whereas total calcium score is more closely associated with the presence and severity

of maximum angiographic stenosis.[32] Detection of coronary calcium by EBCT has been demonstrated to be highly sensitive for the presence of significant CAD. A report of 1764 persons undergoing angiography and EBCT similarly showed a very high sensitivity and negative predictive value in men and women (>99%).[33] Therefore, a calcium score of 0, denoting evidence of coronary calcium, can virtually exclude those patients with obstructive CAD, making this test an effective screen prior to invasive angiography. Guerci et al.[34] studied 290 men and women undergoing coronary arteriography for clinical indications and concluded that EBCT scanning improved discrimination over conventional risk factors in the identification of persons with angiographic coronary disease.

An important point in the interpretation of CAC scores relates to the detection of obstructive CAD. A negative test, indicating no evidence of calcified atherosclerotic plaque, can virtually exclude obstructive disease. A positive EBCT study, indicating the presence of CAC, is nearly 100% specific for atheromatous coronary plaque.[35] However, since both obstructive and nonobstructive lesions have calcification present, CAC is not specific to obstructive disease. While increasing calcium scores are more predictive of obstructive CAD, there is not a 1:1 relationship between calcification and stenosis. The overall specificity of any CAC for obstructive CAD is approximately 66%.[36] In a study of 1851 patients undergoing angiography and CAC measure,[37] EBCT calcium scanning in conjunction with pretest probability of disease derived by a combination of age, gender, and risk factors, could assist the clinician in predicting the severity and extent of angiographically significant CAD in symptomatic patients. Electron beam CT is comparable to nuclear exercise testing in the detection of obstructive CAD.[38,39] As opposed to stress testing, the accuracy of EBCT is not limited by concurrent medications, ability to exercise, or baseline electrocardiogram abnormalities. Moreover, scanning for coronary calcium (CC) does not require injection of contrast medium; therefore, a CT technician can perform the study without supervision. The entire procedure takes less than 10 minutes to perform. However, cardiac CT does not afford assessment of functional status of the patient, so many physicians may utilize a treadmill test and calcium scan together. This algorithm has been shown to improve the diagnostic accuracy of both tests,[40] without significantly increasing cost.

Role of Coronary Calcium in Risk Stratification

Disease processes related to atherosclerosis are the primary cause of morbidity and mortality in every industrialized nation. The initial manifestation of CAD is a MI or death in up to 50% of patients.[41] Most cardiac events occur in the intermediate risk population, where aggressive risk-factor modification is not often recommended or applied. Unfortunately, traditional risk factor assessment helps predict only 60% to 65% of cardiac risk; therefore, many individuals without established risk factors for atherosclerotic heart disease continue to experience cardiac events.[42] Acute coronary occlusion most frequently occurs at the site of mild to moderate stenoses (<50% lesion severity) in association with the process of plaque rupture.[43,44] Therefore, plaque burden, and not stenosis severity, is a more important marker of disease.[45] These studies emphasize the importance of measurement of atherosclerosis burden in the risk stratification for future cardiovascular events, rather than relying solely on evidence of obstructive coronary artery disease.

Coronary Artery Calcium Risk Prediction in Symptomatic Individuals

Studies have demonstrated that CAC has prognostic significance in symptomatic individuals. Margolis et al.[46] assessed the significance of CAC found on fluoroscopy in 800 patients undergoing coronary angiography. The patients with CAC had a 5-year survival rate of 58%, compared with a rate of 87% for the patients without CAC. A study of 192 patients observed for an average of 50 ± 10 months, after undergoing an EBCT study while in the emergency department for chest discomfort, found that the presence of CAC (calcium score >0), and increasing absolute calcium score values were strongly related to the occurrence of hard events ($p < .001$) and all cardiovascular events ($p < .001$).[47] The patients with absolute calcium scores in the top two quartiles had a relative risk of 13.1 (95% CI, 5.6–36; $p < .001$) for new cardiovascular events as compared to patients with lower scores. The annualized cardiovascular event rate was 0.6% for subjects with a coronary artery calcium score of 0 compared with an annual rate of 13.9% for patients with a coronary artery calcium score >400 ($p < .001$).

A multicenter study of 491 patients undergoing coronary angiography and EBCT scanning found that higher calcium scores were associated with a markedly increased risk of coronary events over the next 30 months.[48] In multivariate analysis, the only predictor of a hard cardiac event was log calcium score, even with coronary risk factors and angiographic disease included in the model. In another study of symptomatic patients, EBCT-detected CAC was a stronger independent predictor of disease and future events than a sum of all of the traditional risk factors combined.[49] Keelan et al.[50] followed 288 symptomatic persons who underwent angiography and EBCT calcium scanning for a mean of 6.9 years, and found age and CAC score were the only independent predictors of future hard coronary events.

Coronary Artery Calcium in Asymptomatic Individuals

Coronary artery calcium is also a useful predictor of cardiovascular events in asymptomatic individuals. Unfortunately, at least half of all first coronary events occur in asymptomatic individuals who are unaware that they have developed CAD, and often present as sudden death or acute MI.[45] Several lipid-lowering trials have shown that substantial risk reduction can be attained with both secondary and primary prevention measures.[51]

Several prospective trials have demonstrated the prognostic ability of EBCT to identify asymptomatic patients at high risk of cardiac events. Arad et al.[52] reported 3.6-year follow-up of 1173 patients. Asymptomatic individuals were scanned using EBCT as well as measures of traditional risk factors, and followed prospectively for cardiac events. This study demonstrated CAC to be the strongest predictor of future cardiac events, with patients in the highest score category over 20 times more likely to suffer a cardiac event (odds ratio 22.3, CI 5.1–97.4).

Wong et al.[53] followed 926 asymptomatic patients (mean age 54 years) for an average of 3.3 years. The presence of CAC and increasing score quartiles were related to the occurrence of new MI ($p < .05$), revascularization ($p < .001$) and total cardiovascular events ($p < .001$). The risk ratio for events in patients whose absolute calcium score was in the upper quartile (score > 271) compared with individuals whose absolute calcium score was in the lowest quartile (score < 15) was 12 (relative risk 8.8 and 0.72, respectively; $p < .001$).

Greenland et al.[54] published long-term follow-up of the South Bay Heart Watch. Coronary artery calcium was found to be predictive of risk in patients with a Framingham Risk Score of >10%, with a high CAC score able to predict risk beyond Framingham risk score alone. As compared to a CAC score of 0, a CAC score of >300 was highly predictive of cardiac events (HR 3.9, $p < .001$).

Raggi et al.[55] followed 632 asymptomatic individuals with risk factors for CAD for an average of 32 ± 7 months. A CAC score of zero was associated with a 0.11%/year event rate, compared to 4.8%/year with a score >400. The event rate in patients with calcium scores in the highest quartile was 22 times the event rate in patients with calcium scores in the lowest quartile, significantly outperforming risk factors in cardiac event prediction. Multiple logistic regression analyses demonstrated that calcium score percentile was the only significant predictor of events and provided incremental prognostic value when added to traditional risk factors for CAD.

Larger trials have been reported, demonstrating approximately 10-fold increased risk with the presence of CAC. Kondos et al.[56] reported 37-month follow-up on 5635 initially asymptomatic low- to intermediate-risk adults. In men, events ($n = 192$) were associated with the presence of CAC [relative risk (RR) = 10.5, $p < .001$), diabetes (RR = 1.98, $p = .008$), and smoking (RR = 1.4, $p = .025$), whereas in women events ($n = 32$) were linked to the presence of CAC (RR = 2.6, $p = .037$) and not risk factors.

A prospective study of 5585 subjects aged 59 ± 5 years, a calcium score ≥100 predicted all atherosclerotic cardiovascular disease events, all coronary events, and the sum of nonfatal MI and coronary death events with relative risks of 9.5 to 10.7 at 4.3 years.[57] The calcium score also predicted events independently of and more accurately than measured risk factors. The area under the receiver operating characteristic curve for event prediction with risk factors alone in this study was 0.71, increasing to 0.81 with EBCT testing ($p < .01$). This prospective study strongly demonstrated the ability to utilize this test to rule out patients who do not require therapy. In this study, only 19% of patients had scores above the diagnostic threshold (calcium score ≥100), yet relying on this threshold had a negative predictive power of 99.2%. Thus, clinicians can focus on a smaller, yet higher risk population (10.7-fold increased risk in this group), for risk reduction therapy.

Shaw et al.[58] demonstrated the power of coronary artery calcium to predict all-cause mortality over the next 5 years. A cohort of 10,377 asymptomatic individuals undergoing cardiac risk factor evaluation and CAC measure with EBCT reported a mean follow-up of 5.0 years. In a risk-adjusted model, CAC was an independent predictor of mortality ($p < .001$). Coronary calcium was a better predictor than traditional cardiovascular risk factors, and very high scores (>1000) were associated with a 13-fold increased risk of death as compared to persons with lower scores.

Coronary Artery Calcium: Guidelines and Applications

The above-mentioned studies demonstrate the ability of CAC to provide risk stratification in asymptomatic and symptomatic populations with incremental prognostic information beyond traditional risk factors. Based on the results of these studies, modification of the Framingham Global Risk Score by using a weighted factor based on the patient's individual calcium score percentile has been suggested.[59] In this modification, the Framingham Risk Score assigned to a subject undergoing EBCT screening for asymptomatic CAD is increased if the calcium score is in a high percentile.

The greatest potential for CAC detection could be as a marker of CAD prognosis in asymptomatic persons at risk of CAD, beyond that detected by conventional coronary risk factors. Since the 2000 American College of Cardiology (ACC)/American Heart Association (AHA) expert consensus document on EBCT noting inconclusive risk stratification evidence on CAC scanning,[60] a number of studies have reported that the presence and severity of CAC has independent and incremental value when added to clinical or historical data in the measure of death or nonfatal MI. Since those early recommendations, the National Cholesterol Education Program (NCEP) has made recommendations specifically for the use of EBCT to assist in risk stratification in elderly and intermediate risk patients. The new NCEP guidelines (Adult Treatment Panel III)[61] support the conclusions of the AHA's Prevention Conference V[62] and the ACC/AHA report[60] that high coronary calcium scores signify and confirm increased risk for future cardiac events, and state, "Therefore, measurement of coronary calcium is an option for advanced risk assessment in appropriately selected persons. In persons with multiple risk factors, high coronary calcium scores (e.g., >75th percentile for age and sex) denotes advanced coronary atherosclerosis and provides a rationale for intensified LDL-lowering therapy." New guidelines for prevention of CAD recommend coronary calcium as a method of risk stratification, with positive scores placing individuals at intermediate risk by the Framingham model (10–20% 10-year risk) and high CAC scores at high risk for future cardiac events.[63]

The absence of CAC in the asymptomatic patient identifies a group of patients at very low risk of events over the next 3 to 5 years. An annual event rate of only 0.11% has been reported for patients with scores of zero.[55] Both the ACC/AHA writing group and the Prevention V Conference agreed that the negative predictive value of EBCT is very high for short-term events.[60,62] Whether a calcium score of zero will allow therapy to be withheld remains to be prospectively tested.

Current guidelines suggest that intermediate risk patients would benefit most from further risk stratification, as most cardiac events occur in this population.[61] "Recent work suggests that electron-beam tomography (EBCT) can also improve risk prediction in intermediate-risk patients. Thus, with a prior probability of a coronary event in the intermediate range (>6% in 10 years but <20% in 10 years), a calcium

score would yield a posttest probability in virtually all such patients greater than 2% per year, that is, a level similar to that in secondary prevention, or a "coronary risk equivalent." Furthermore, CAC screening with EBCT was demonstrated to be a cost-effective screening strategy in asymptomatic individuals between 45 and 65 years of age.[64] The ability of CAC scoring to identify patients who require aggressive risk factor modification, coupled with effectiveness of cholesterol lowering medications, aspirin, and other therapies, should allow physicians to focus aggressive preventative treatment on those individuals with underlying atherosclerosis who are at highest risk of having cardiovascular events.

There are some potential specific applications of CAC assessment that warrant mention. Based on the fact that a CAC score of zero is associated with a <1% chance of obstructive CAD, the use of EBCT prior to angiography has been recommended for certain persons of low-to-intermediate risk of obstructive CAD. In the symptomatic patient, evidence suggests that calcium scanning may be more cost-effective at diagnosing CAD than traditional noninvasive testing, especially in women.[64,65,66]

Another potential application of cardiac CT relates to the triage of chest pain patients. Electron beam CT has been shown to be an efficient screening tool for patients admitted to the emergency department with chest pain to rule out myocardial infarction.[47,67,68] These studies demonstrate sensitivities of 98% to 100% for identifying patients with acute MI, and very low subsequent event rates for persons with negative tests. The high sensitivity and negative predictive value may allow early discharge of those patients with nondiagnostic ECG and negative calcium scans. Exclusion of coronary calcium, therefore, may be used as an effective screen prior to invasive diagnostic procedures or hospital admission.

In patients with cardiomyopathy, CAC has been shown to be useful in determining the etiology of cardiomyopathy. The clinical manifestations of patients with ischemic cardiomyopathy are often indistinguishable from those patients with nonischemic dilated cardiomyopathy. Budoff et al.[69] demonstrated in 120 patients with heart failure of unknown etiology that the presence of CAC was associated with a 99% sensitivity for ischemic cardiomyopathy.

Electron Beam versus Multidetector CT for Assessment of Coronary Artery Calcium

The higher tube currents available with MDCT allow for images with a better signal-to-noise ratio and higher spatial resolution in comparison to EBCT, but at the expense of higher radiation exposure and lower temporal resolution. Retrospective gating involves acquiring hundreds of cardiac image, but only uses those that occurred with appropriate diastolic timing. This retrospective approach markedly increases the radiation dose, image analysis time, inter- and intra-reader variability, and interscan variability. A more practical approach is prospective gating, which is similar to the methods employed by EBCT. This methodology allows for image acquisition only at the specified time (diastole), and therefore reduces variability and radiation. For MDCT, the images are best when the resting heart rate is less than 60 beats per minute; at faster heart rates, motion artifacts may become more prominent.

Protocols are being developed that may reduce radiation doses with MDCT, by attempting to decrease beam current during systole, when images are not used for interpretation. New AHA guidelines are being published discussing the advantages and disadvantages of each modality.[70] These guidelines conclude that "some limitations remain for multidetector CT, including: (1) slower speed of the acquisition (EBCT = 50–100 msec, MDCT = 200–330 msec); (2) higher radiation dose (EBCT dose = 0.7 mSv, MDCT dose = 1.5–1.8 mSv); and (3) possibly greater interscan variability of measurement (EBCT = 11–16%, MDCT = 23–35%)." Two ongoing trials [multi-ethnic study of atherosclerosis (MESA) trial in the United States and the Heinz Nixdorf Recall Study in Germany] are examining the value of EBCT and/or MDCT-derived CAC in the general population, and will provide more answers in relation to the role of CAC in the primary prevention of atherosclerosis.

Position of the Professional Societies and Guidelines

In 1996, the AHA assembled a writing group on the application of EBCT coronary calcium scanning. This group concluded that EBCT CAC was a useful surrogate for atherosclerosis, with a negative test most likely associated with normal coronary arteries and a low risk of cardiac events in the next 2 to 5 years, and a positive test being associated with atherosclerosis.[33]

Fortunately, the AHA and the ACC have taken responsible positions on this issue. Given the strong literature in support of risk stratification with this tool, the issue of CAC scanning is undergoing a current revision and should have stronger support from both organizations, especially given the incremental and independent predictive value found in all studies to date.

Recent guidelines and expert consensus documents have recommended the use of CAC (or the use of other tests of atherosclerosis burden) in clinically selected intermediate CAD risk patients (e.g., those with a 10% to 20% Framingham 10-year risk estimate) to refine clinical risk prediction[62,71,72] and to select patients for altered targets for lipid-lowering therapies.[61,73]

Contrast-Enhanced Computed Tomography Angiography

Electron Beam Angiography

The ability to visualize the coronary artery lumen has revolutionized CT imaging. An alternative, less expensive, and noninvasive test for use as a diagnostic tool before possible intervention could have a major impact on health care practice and cost containment.[4] Contrast-enhanced CT angiography is an emerging technology with the potential for obtaining essentially noninvasive coronary arteriograms. Studies have reported contrast-enhanced, electrocardiogram (ECG)-triggered, 3D-EBCT angiography for detecting and grading coronary stenosis.[74,75,76,77,78,79] Coronary electron beam angiography (EBA) was first introduced in 1995,[80] and since

that time has improved due to technology and methodology advances. Electrocardiogram triggering is employed, so that each image is obtained at the same point in diastole. Iodinated contrast is administered through an antecubital or jugular vein with an injection rate of approximately 4 mL/sec and total volume of 80 to 160 mL, depending on the version of scanner used. Images are obtained over a single breathhold, usually over approximately 30 seconds. This entire protocol can be performed within 15 to 20 minutes. Image processing is rapid, with detailed analysis through the assessment of two-dimensional (2D) and 3D views as well as maximum intensity projections in which serial overlapping thin slices are viewed in unison (Figs. 8.3 to 8.5).[81] As compared to invasive angiography, this modality has been demonstrated to identify significant coronary lumen narrowing (>50% stenosis) with an overall sensitivity of 87% and specificity of 91% for the 10 or so studies now reported.[4]

These early studies, while demonstrating sensitivities and specificities in the range of 88% to 94%, were somewhat limited by nonevaluable segments, despite the high temporal resolution of EBCT (100-ms imaging). Historically, the most common trigger time used is 80% of the R-R interval. However, this trigger occurs on or near the P wave during atrial systole. Electrocardiogram triggering at 80% of the R-R interval (late diastole) used in most prior studies might not be optimal for imaging of the coronary segments near the right or left atria, since atrial contraction during end-diastole causes rapid movement of the base of the heart,[82] and the least motion among all heart rates occurs earlier in the cardiac cycle (late systole).[83] A study was subsequently reported demonstrating a marked improvement in results with EBCT when using end-systolic triggering rather than late diastolic triggering.

Lu et al.[84] studied 133 patients with suspected coronary disease with intravenous coronary EBA and conventional coronary angiography. Patients were divided into two groups based on different ECG triggering used: 80% R-R interval trigger method (group 1, $n = 53$) and end-systolic triggering (group 2, $n = 80$). Overall sensitivity (including all segments, not just evaluable segments) to detect a ≥50% luminal stenosis was 69% in group 1 and 91% in group 2 ($p = .002$); specificity was 82% and 94% in group 1 and group 2, respectively ($p < .001$). Nonassessability of coronary segments on 3D-EBA images was reduced from 35% in group 1 to 9% in group 2 patients ($p < .001$). The number of motion-free coronary images increased from 67% to 95% from group 1 to group 2 ($p < .0001$).

Another study by Budoff et al.[85] reported the improvement with image quality and diagnostic accuracy with newer triggering techniques was also reported. Eighty-six patients

FIGURE 8.4. Electron beam angiography demonstrating the obtuse marginal (OM) and circumflex without evidence of obstructive coronary artery disease.

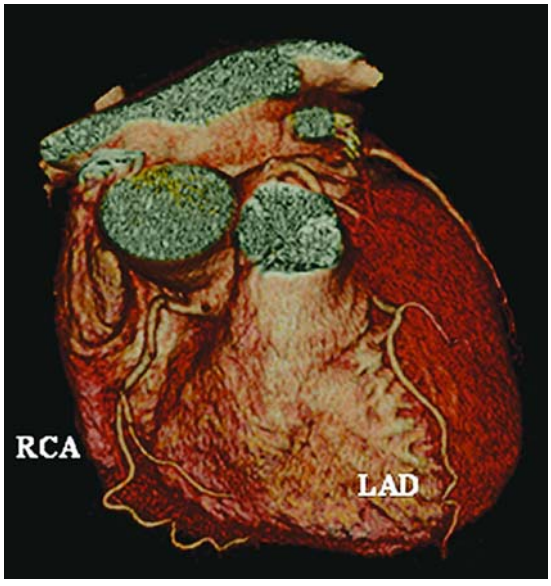

FIGURE 8.3. E-Speed (General Electric, San Francisco, CA) electron beam angiography demonstrating the left and right coronary arteries, without evidence of obstructive coronary artery disease. LAD, left anterior descending coronary artery; RCA, right coronary artery.

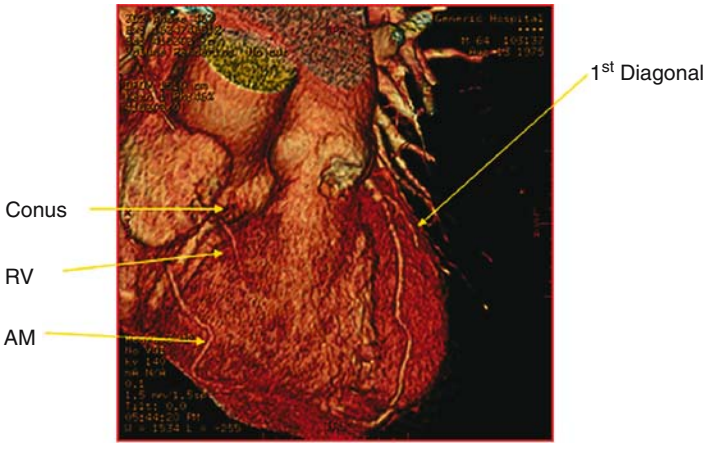

FIGURE 8.5. Computed tomography angiography demonstrating the left and right coronary arteries, without evidence of obstructive coronary artery disease. The conus artery, as well as the right ventricular vein and acute marginal branches are well visualized. 1st Diag, first diagonal artery; AM, acute marginal branch of right ventricle; RV, right ventricular vein.

were studied; EBT correctly classified 49 of 53 patients (92%) as having at least one coronary stenosis. Overall, 103 stenoses exceeding 50% diameter reduction were present, and of these 93 lesions were correctly detected by EBT (sensitivity: 90%; specificity: 93%; positive predictive value: 84%; and negative predictive value: 96%). Only 5% of vessels could not be assessed, predominantly due to significant calcification.

Newer advances in both modalities will lead to routine use of noninvasive angiography. In regard to the EBCT scanner, newer electron beam technologies are now available (e-speed, General Electric, San Francisco, CA) that provide greater spatial and temporal resolution and may provide greater visualization of smaller branch veins as well as distal tapering sections of branch veins than the scanner used in this study.[86] Early results from this scanner demonstrate sensitivities of 92% and specificities of 98% for the detection of obstructive CAD.[87]

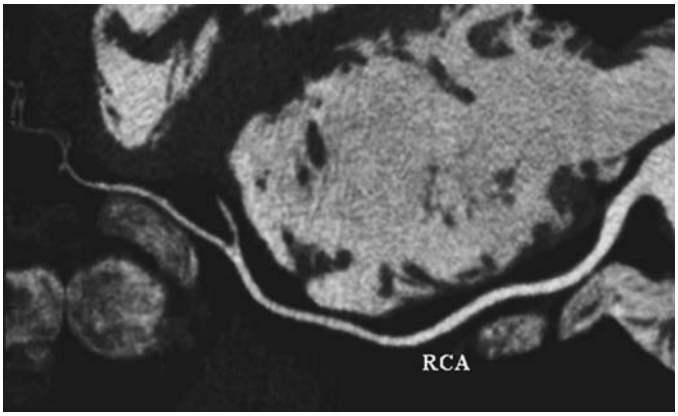

FIGURE 8.6. Quantum 64 (Toshiba Medical Systems) multidetector CT image demonstrating a multiplanar reconstruction of the right coronary artery (RCA). This allows the entire vessel to be viewed in one image.

Multidetector Computed Tomography Angiography

Multiple studies with four-slice MDCT have been reported, with most studies reported a diminished overall sensitivity. Achenbach et al.[88] reporting 68% of vessels interpretable by angiography, with 32 of 58 high-grade stenoses were detected (sensitivity 55%). All four major coronary arteries could be evaluated in only 30% of patients. The authors note that "its clinical use may presently be limited due to degraded image quality in a substantial number of cases, mainly due to rapid coronary motion." Giesler et al.[89] reported that 115 of 400 (29%) coronary arteries were uninterpretable, and in only 39% of patients were all coronary arteries assessable by MDCT. Overall, 51 (49%) of 104 stenoses were revealed on MDCT. Additionally, most studies demonstrate a significant heart rate interaction. One study demonstrated that overall sensitivity for stenosis detection decreased from 62% (heart rate <70 bpm) to 33% (heart rate >70 bpm),[89] while in another sensitivity dropped from 82% (mean heart rate 55.8 bpm) to 32% (mean heart rate 81.7 bpm).[90]

The use of eight or more detectors improves spatial resolution by decreasing slice thickness, and it allows for a higher sensitivity and specificity. Average sensitivity and specificity over the first six studies reported an average sensitivity of 80% and specificity of 86%, when including all segments for analysis.[91] Excluding those with motion artifacts and other reasons for nonassessability increases the sensitivity and specificity to approximately 90%. The use of eight 64-slice MDCT scanners allows for faster and thinner imaging than the four-slice scanners (Figs. 8.6 to 8.8). Three studies have recently been reported with 16-level scanners,[92,93,94] each with improved accuracy as compared to prior reports with 4-level scanners. These studies reported a sensitivity of 73% to 95% and a specificity of 86% to 93%. The most recent study was a prospective, blinded, standard cross-sectional technology assessment; analysis of all 530 coronary segments demonstrated moderate sensitivity (63%) and excellent specificity (96%), with a moderate positive predictive value of 64% and an excellent negative predictive value of 96% for the detection of significant coronary stenoses. Assessment restricted to either proximal coronary segments or segments with excellent image quality (83% of all segments) led to an increase in sensitivity (70% and 82%, respectively), and high specificities were maintained (94% and 93%, respectively).

These studies concluded the MDCT with beta-blocker premedication permits detection of CAD with improved accuracy. When using MDCT as a noninvasive diagnostic

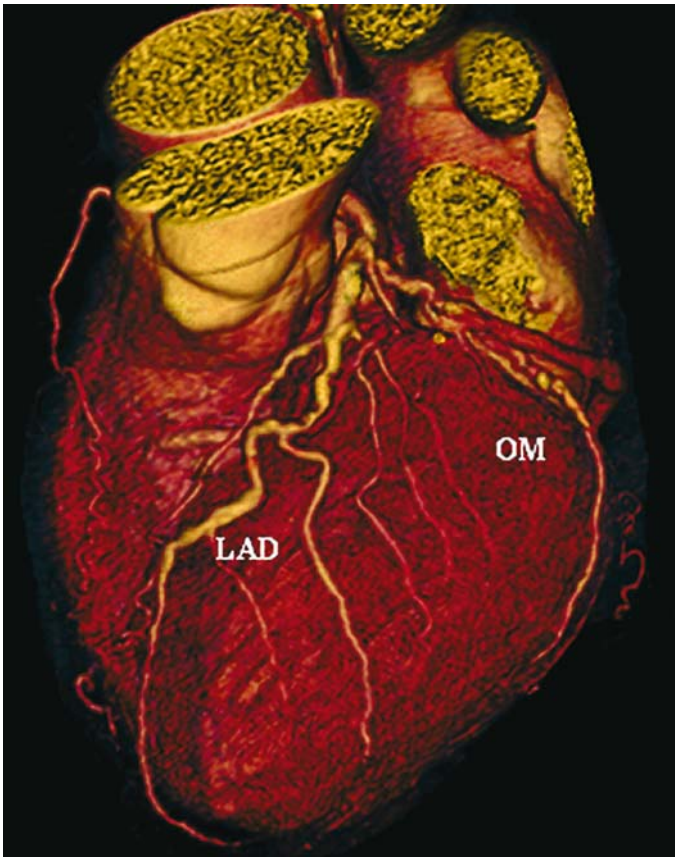

FIGURE 8.7. Volume rendered image of the left coronary system using a Lightspeed 16 multidetector computed tomography (General Electric, Milwaukee, WI) demonstrating mild, nonobstructive disease. LAD, left anterior descending artery; OM, obtuse marginal.

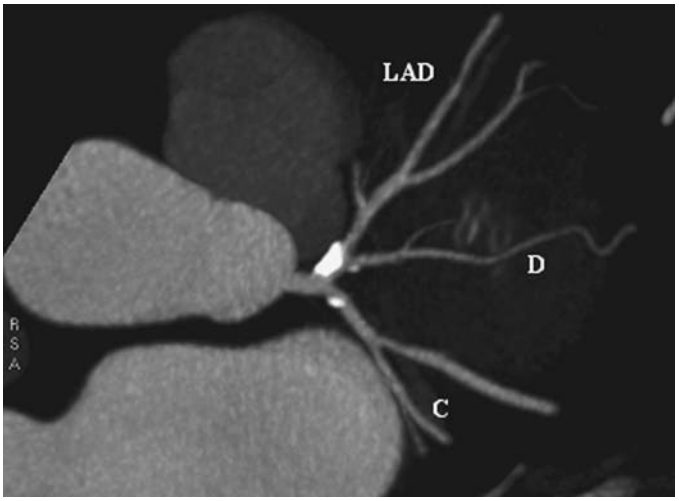

FIGURE 8.8. Maximal intensity projection demonstrating significant disease at the origin of the left anterior descending artery (LAD). C, circumflex coronary artery; D, diagonal.

modality to assess advanced CAD, it appears to be mandatory to preselect patients (sinus rhythm, lower calcium score, steady heart rates) in order to achieve reliable results, and to use scanners with eight or more detectors.

Computed Tomography Angiography after Revascularization

Computed tomography angiography may play a role in the assessment and follow-up of patients who have undergone coronary interventions, potentially replacing some invasive angiographic procedures. The utilization of EBA to detect coronary artery bypass graft (CABG) patency has been reported as early as 1986.[95] Saphenous vein grafts, which are generally of large caliber and have minimal cardiac motion, are especially well suited for noninvasive imaging with CT angiography (Figs. 8.9 and 8.10). Using 3D visualization in post-CABG patients, both MDCT and EBCT can demonstrate graft stenosis and patency. Recent studies for both CT techniques demonstrate sensitivities of 92% to 100% and specificities of 91% to 100% for establishing patency of saphenous vein grafts as compared to coronary angiography.[96,97,98] These studies demonstrated sensitivity and specificity for patency of left internal mammary of 80% to 100% and 82% to 100%, respectively.

In patients who experience chest pain after stenting or angioplasty, visualization of the site of angioplasty to assess for restenosis is often required. A noninvasive method to visualize the site of angioplasty could potentially be used for less typical presentations of acute closure (no typical angina or ECG changes suggestive of ischemia). Computed tomography angiography has been shown to permit imaging of the coronary arteries and detecting high-grade restenosis after coronary angioplasty. Achenbach et al.[99] reported 50 cases in which a coronary angioplasty was performed without coronary stent implantation. The sensitivity and specificity of EBA was 94% and 82%, respectively, to detect severe stenosis (≥70% stenosis). The widespread utilization of metal stents during revascularization procedures provides a major limitation for the clinical assessment of the according arterial segment by EBA, MDCT, and MR angiography. Pump et al.[100] reported a sensitivity of 78% (18 of 23 stenoses detected) and specificity of 98% (189 of 193 stents correctly assessed to be

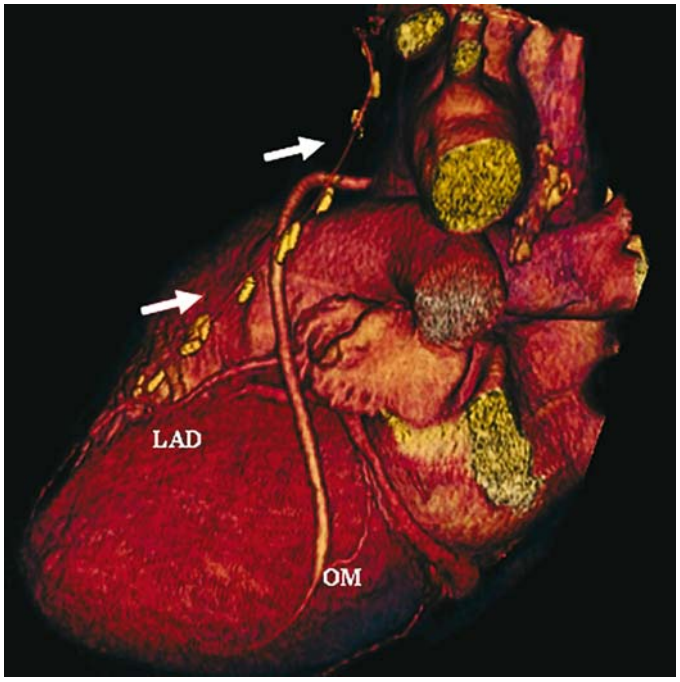

FIGURE 8.9. Noninvasive angiography demonstrating patent saphenous vein grafts to the first obtuse marginal (OM) and a patent internal mammary artery (white arrows) to the left anterior descending coronary artery (LAD).

FIGURE 8.10. Noninvasive angiography demonstrating multiple closed saphenous vein grafts (black arrows) and a right coronary artery (RCA) occlusion with a patent saphenous vein graft to the left anterior descending artery (white arrow).

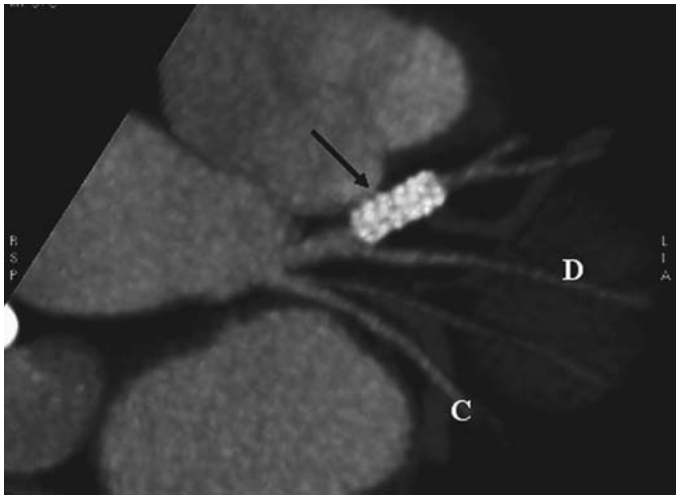

FIGURE 8.11. Noninvasive angiography using the Lightspeed 16 multidetector computed tomography demonstrating a stent (black arrow) in the left anterior descending. It is not possible to determine whether the stent is patent or partially occluded.

free of stenosis) for the detection of significant in-stent restenosis by flow measurements. The difficulties in imaging stents (with scatter from the metal, coupled with motion artifacts and small interior diameters) make CT angiography very limited in this application currently (Fig. 8.11).[101] Although some authors have reported mixed results with CT imaging within stents, current studies are limited, and the scatter artifact of the metal, coupled with the small diameters and coronary motion, suggest that invasive coronary angiography is required to evaluate stent patency accurately.

Assessment of Noncalcified Plaque

Computed tomography angiography's ability to visualize and characterize "soft" noncalcific coronary plaque is an emerging area of interest (Fig. 8.12). Autopsy and coronary intravascular ultrasound (IVUS) studies have shown that angiographically "normal" coronary artery segments may contain a significant amount of atherosclerotic plaque;[102] IVUS allows for a direct, 360-degree visualization of the coronary atheroma within the vessel wall and identifies both plaque distribution and composition.[103] The utility of coronary IVUS over coronary angiography in recognizing these smaller plaques is somewhat limited, though, by a higher procedural complication rate secondary to its more invasive nature.

The potential identification of early, nonobstructive coronary plaques with CT angiography requires further investigation. The noncalcified "soft" plaque in coronary arteries is measured as the volume under 130 HU on nonenhanced images corresponding to filling defects on enhanced images. The noncalcified plaque can be divided into low (<0 HU) and higher-density noncalcified plaques (0–130 HU). A comparison study with EBCT and IVUS demonstrated a linear relationship between coronary segments with calcified and with noncalcified plaques.[104] In comparisons of MDCT with IVUS, investigators found a sensitivity of 82% to detect coronary artery segments containing atherosclerotic plaque in patients without significant coronary artery stenoses.[105,106] However, segments containing exclusively noncalcified plaque were identified with a sensitivity of only 53%, and MDCT substantially underestimated plaque burden. Accuracy for plaque detection was lower for smaller plaques and in distal versus proximal vessel segments.

The limitations of soft plaque detection may be much more significant than a limited sensitivity or underestimation of plaque burden. The reproducibility of the measure has not been reported. Additionally, there are no prognostic data assessing whether noncalcific plaque adds any prognostic information to traditional risk factors, angiographic disease severity, and calcified plaque quantitation. Finally, this procedure requires both contrast and radiation, and the risks may outweigh the benefit in individual patients. These factors require further investigation in order to define the possible role and importance of CT coronary angiography as a noninvasive modality for soft plaque imaging.

Radiation Dose and Cardiac CT

Computed tomography utilizes x-rays, a form of ionizing radiation, to produce the information required for generating CT images. One drawback of MDCT as compared to EBCT is the potential for higher radiation exposure to the patient, depending on the tube current selected for the examination. Hunold et al.[6] recently performed a study of radiation doses during cardiac exams. Cardiac scanning was performed with EBCT and four-slice multidetector CT (Siemens Volume Zoom, Ehrlangen, Germany) utilizing prospective triggering to assess patient effective radiation exposure, compared to measurements made during cardiac catheterization.

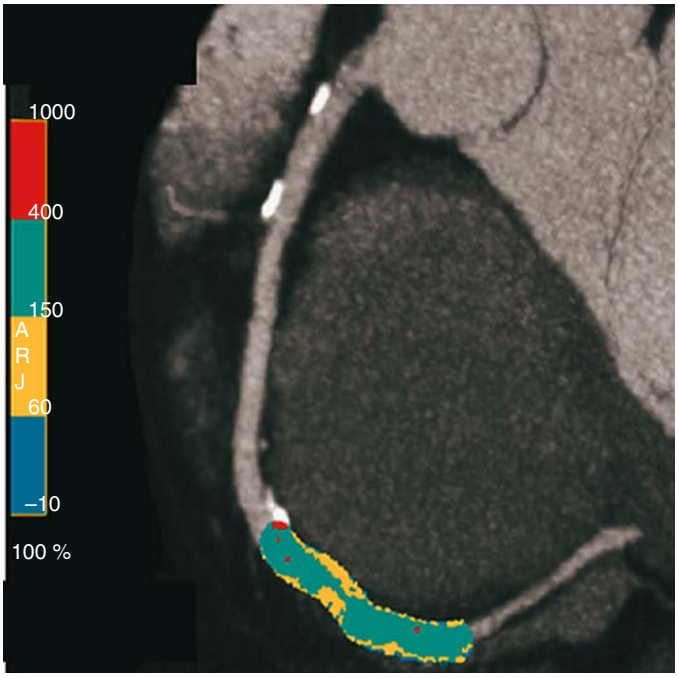

FIGURE 8.12. Noninvasive angiography with significant stenosis consisting of noncalcified plaque (depicted as yellow) in the distal right coronary artery. The red structures represent calcium and the green is the contrast.

Electron beam CT CAC protocols yielded effective doses of 1.0 and 1.3 mSv for men and women, while MDCT CAC protocols using 100 mA, 140 kV, and 500-ms rotation yielded 1.5 mSv for men and 1.8 mSv for women. Invasive coronary angiography yielded effective doses of 2.1 and 2.5 mSv for men and women, respectively. The doses obtained for MDCT angiography were significantly higher. Since radiation is continuously applied (retrospective gating) while only a fraction of the acquired data is utilized, high radiation doses (doses of 6 to 10 mSv/study) still limit the clinical applicability of this modality.[6,107] In females, the effective radiation doses is another 25% higher than in males, raising the mean dose from 8 mSv in men to 10 mSv per study in women.[108] These radiation doses are two to five times higher than can be expected for conventional angiography, and five- to tenfold higher than doses obtained during EBCT angiography (1.1–1.7 mSv). In two studies of radiation dose comparing EBCT and four-slice MDCT, the first reported EBCT angiography doses of 1.5 to 2.0 mSv, MDCT angiography 8.1 to 13 mSv, and coronary angiography 2.1 to 2.3 mSv, while another reported EBA doses of 1.1 mSv and MDCT doses of 9.3 to 11.3 mSv.[6,109] Newer MDCT studies report that radiation doses are still significant with newer 16+-level multidetector scanners,[110] and dose modulation should be employed whenever possible.[111]

For MDCT, increased numbers of detectors (64-slice systems are now available) will allow for better collimation and spatial reconstructions. Having more of the heart visualized simultaneously will also allow for reductions in the contrast requirements and breath holding, further improving the methodology. Multisector reconstruction (combining images from consecutive heart beats) and dose modulation (to reduce radiation exposure during systole, when images are not used for reconstruction) are increasingly being applied.

Limitations of CT Angiography

Some limitations are inherent to both CT modalities in regard to coronary artery imaging. One major limitation is dense calcification of the coronary arteries, with investigators citing scores of >500 or >1000 as problematic. Another limitation of all noninvasive angiography is the relative inability to visualize collaterals. The main determinant of false-positive results for diagnosing ≥50% coronary luminal stenosis was small vessel size, and the diameter of stenotic segments tends to be underestimated by CT angiography.[112]

Applications of CT Coronary Artery Angiography

The most common clinical application of CT angiography is to evaluate patients with symptoms post-CABG surgery and coronary angioplasty evaluation, assessment of congenital heart disease and coronary anomalies,[113] and measurement of wall motion, myocardial mass, as well as right and left ejection fractions.[114]

Some current uses of noninvasive CT angiography include the following: after the nondiagnostic stress test; for those persons with intermediate likelihood of CAD (where the step to coronary angiography might be premature); for symptomatic persons postcoronary angioplasty and possibly poststent; evaluating graft patency post-CABG; and for early detection of obstructive CAD in the high-risk person. Given the current utility of these techniques, we can expect a rapid growth in both the knowledge and experience with noninvasive angiography, leading to much wider clinical applications for the assessment of obstructive coronary artery disease.

Ventricular Structure and Function

Advances in image acquisition and data processing have allowed for characterization of ventricular structures and function with CT angiography, with reproducible quantitative measurement of left ventricular ejection fraction,[115,116] ventricular volumes,[117,118] ventricular mass,[119,120] wall thickness,[121] and regional wall motion[122] in cardiomyopathic processes (Fig. 8.13). These data can be integrated with coronary artery assessment for a comprehensive assessment of the role that coronary artery disease plays in the cardiomyopathic process.

Cine scanning allows for assessment of systolic and diastolic function. The spatial resolution and contrast enhancement adequately defines the endocardium of both the right and left ventricles, so that precise measurement of biventricular cardiac volume and ejection fraction is feasible. Rumberger et al.[123] have demonstrated the feasibility of evaluating diastolic performance of the LV. Diastolic filling variables, such as those measured by blood pool scintigraphy, can be determined with EBCT. Application of this technique may prove useful for detecting subtle changes in LV diastolic function induced by myocardial ischemia.

Left ventricular mass can also be quantified. Quantitative measurement of regional wall motion and wall thickening can be performed, which is particularly useful for evaluating CAD patients. Application of this technique may prove useful for detecting changes in LV function induced by myocardial ischemia, as well as accurately diagnosing ejec-

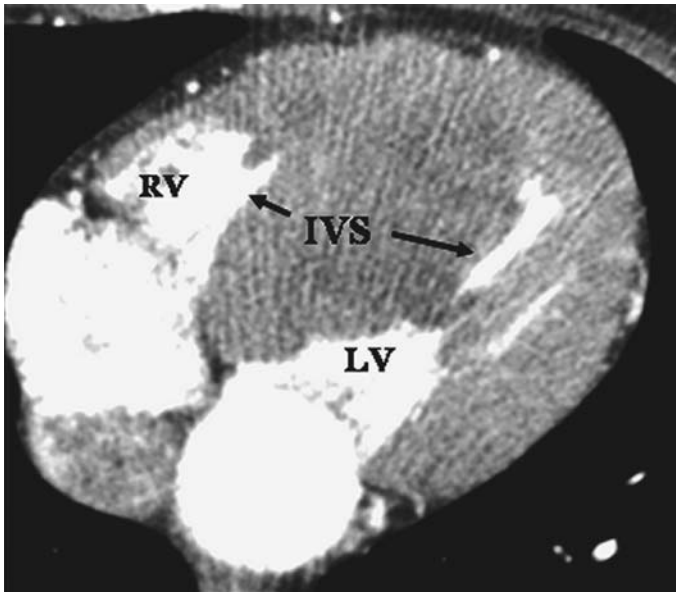

FIGURE 8.13. Profound thickening of the interventricular septum (IVS) in a patient with hypertrophic cardiomyopathy.
LV, left ventricle; RV, right ventricle.

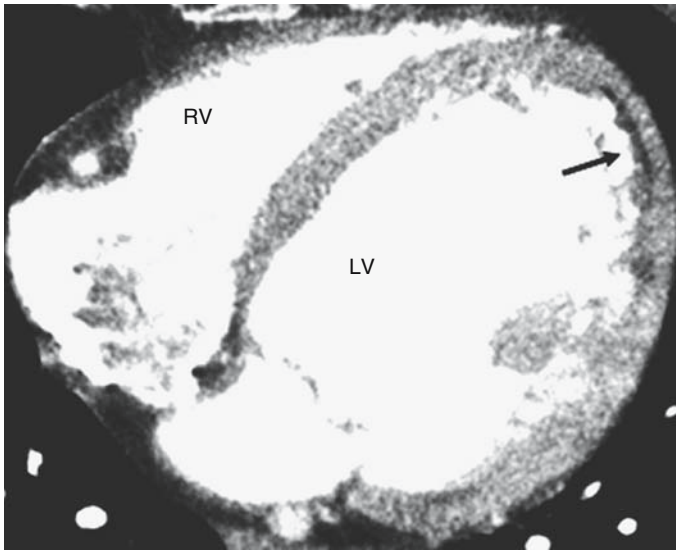

FIGURE 8.14. Severely dilated left ventricle (LV) in a patient with ischemic cardiomyopathy. The apical-lateral infarction can be well visualized by the dark region (lower contrast enhancement due to infarcted tissue, black arrow). RV, right ventricle.

tion fraction postinfarction.[124] Bicycle exercise can be coupled with CT scanning to detect exercise-induced ischemia. A decrease in ejection fraction and development of a new wall motion abnormality have been shown to be accurate for detection of ischemia, with data indicating that exercise CT may be at least as sensitive and more specific than technetium-99m sestamibi stress testing.[125] A study was reported evaluating the diagnostic value of dobutamine stress EBCT as compared with exercise stress thallium-201 single-photon emission computed tomography and found comparable sensitivity and specificity for the detection of myocardial ischemia.[126]

Noninvasive quantitation of myocardial blood flow is also possible by evaluating flow patterns of iodinated contrast on CT. Myocardial blood flow is proportional to the peak iodine concentration in the myocardium after intravenous injection of contrast medium. The technique is accurate for myocardial flows up to 2 mL/min/g. Technical factors related to Compton scatter and beam hardening may cause inaccuracies. Further research is necessary, for the development of clinically useful methods for accurate quantification of blood flow measurements. Based on the principle that blood flow is proportional to iodine concentration during contrast medium infusion, acute MI can be imaged by CT as a region of little or no iodine (low density, Fig. 8.14). This technique has been used to detect MI and to quantitate the infarct size as well as the patency of the infarct vessel, using both flow and 3D techniques. Complications of myocardial infarction, including ventricular septal defects, thrombi, aneurysms, and pericardial effusions, can all be easily visualized by CT.

The ability to document abnormalities of ventricular structure and function coupled with the ability to assess coronary artery calcium and angiographic coronary artery disease make cardiac CT a useful tool in the assessment of cardiomyopathic processes. Definition of the etiology of cardiomyopathy, to quantitate function, can facilitate decision making as well as approaches to intervention in patients with dilated and ischemic cardiomyopathy.

Hypertrophic cardiomyopathy can lead to heart failure symptoms and sudden cardiac death.[127] Echocardiography is the main diagnostic modality for the diagnosis of hypertrophic cardiomyopathy, and in addition to anatomy can assess resting and exercise gradients and associated valve function.[128] The diagnosis can be made by CT angiography (Fig. 8.13)[129,130] and MRI,[131] which can provide details of regional wall thickness, indexed ventricular mass, and ejection fraction.

Assessment of right ventricular structure and function abnormalities has risen in importance due to the recognition of significant disease processes involving the right ventricle. Visualization and assessment of right ventricular function is difficult by echo and cardiac catheterization. Computed tomography angiography potentially may be an effective tool for assessment of right ventricular anatomy and function.[132] Right ventricular pathology, such as right ventricular dysplasia, can be difficult to diagnose, and often the initial presentation is sudden death. In terms of visualization of right ventricular abnormalities, echocardiography lacks sensitivity.[133] Magnetic resonance imaging has been the modality of choice for anatomic evaluation of right ventricular dysplasia due to its superior ability to define tissue characteristics such as myocardial fat deposits, but the variation in fat content and location in patients without this process makes this criterion only of modest clinical utility.[134] Computed tomography angiography has been assessed for the ability to diagnose anatomic features associated with right ventricular dysplasia, such as epicardial and myocardial fat, low-attenuation trabeculations, and right ventricular free wall scalloping, but has not been assessed as a screening tool.[132,135,136]

Cardiac CT can provide excellent depiction of ventricular aneurysms and pseudoaneurysms (Fig. 8.15). The 3D aspects

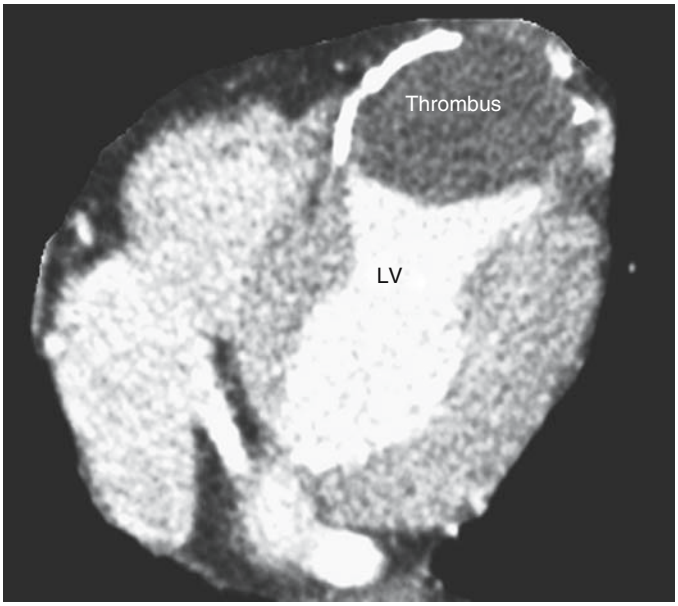

FIGURE 8.15. A patient with a transmural apical infarction demonstrating a large thrombus in the apex. The white structure surrounding the thrombus is calcified myocardium replacing normal tissue after a large infarction. LV, left ventricle.

of the aneurysm can be determined, and global and regional function assessed. Ventricular thrombus can also be easily identified. There is some evidence indicating that CT is more sensitive in detecting LV thrombus than transthoracic echocardiography.[137]

Pericardial Disease

The combination of excellent spatial resolution, tomographic format, and exquisite density differentiation makes EBCT an ideal tool for diagnosis of pericardial disease. Because the normal pericardium is 1 to 2 mm thick, spatial resolution must be very good for any imaging technique to define this structure. X-ray CT is aided by the fact that epicardial and extrapericardial fat often outline the normal pericardium. Fat, being of very low density, serves as a natural contrast agent. Therefore, even minimal pericardial thickening (4 to 5 mm) is well recognized by cardiac CT (Fig. 8.16).[138] The high density of pericardial calcium makes its detection easy. The 3D representation of anatomy by CT provides the surgeon with precise detail of the extent of calcification and the degree of myocardial invasion.

In addition to providing an excellent description of the anatomy of pericardial constriction, EBCT also defines the degree of hemodynamic abnormality by describing diastolic filling from ventricular volume measurements every 50 ms throughout diastole.[123] Cine mode images of the right atrium and RV can also detect diastolic collapse when pericardial tamponade is present. Enlargement of the superior and inferior vena cavae can also be identified when either constriction or tamponade is present. Pericardial effusion is easily detected by CT. Occasionally, very small effusions cannot be distinguished from pericardial thickening, as the CT densities are similar. However, pericardial fluid, if free in the pericardial space, appears as layers, making differentiation from pericardial thickening relatively simple.

Cardiac CT is an excellent diagnostic technique for evaluation of pericardial cysts and tumors.[139] Because CT images the entire thorax and provides clear definition of mediastinal structures, pericardial involvement by metastatic tumors is easily identified. Congenital anomalies, such as absence of the left hemipericardium, are well seen by this modality.

Aorta and Aortic Valve Pathology

Computed tomography angiography can diagnose aneurysm, dissection, and wall abnormalities such as ulceration, calcification, or thrombus throughout the full length of the aorta as well as involvement of branch vessels. The superior temporal and spatial resolution of cardiac CT significantly improves imaging of the aorta, because motion artifacts are eliminated. Computed tomography is a superior method for identification of aortic dissection (Fig. 8.17).[140] The intimal flap is usually well delineated, even in branches of the aorta. In the flow mode, flow can also be assessed in the true and false lumina.

Cardiac CT is also an effective method of imaging aortic aneurysms throughout the extent of the aorta (Fig. 8.18). It is particularly useful for imaging ascending aortic aneurysms before and after surgical treatment. Accurate measurements of aortic root diameter can be made easily and the extent of the aneurysm defined. The origin of the coronary arteries is also well visualized. Thrombus within any aortic aneurysm is easily identified by differences in tissue density during contrast enhancement. The tomographic format of CT provides excellent definition of the relationship of aortic aneurysms to adjacent structures. Leakage of blood from the aneurysm may be recognizable with contrast enhancement of surrounding tissues.

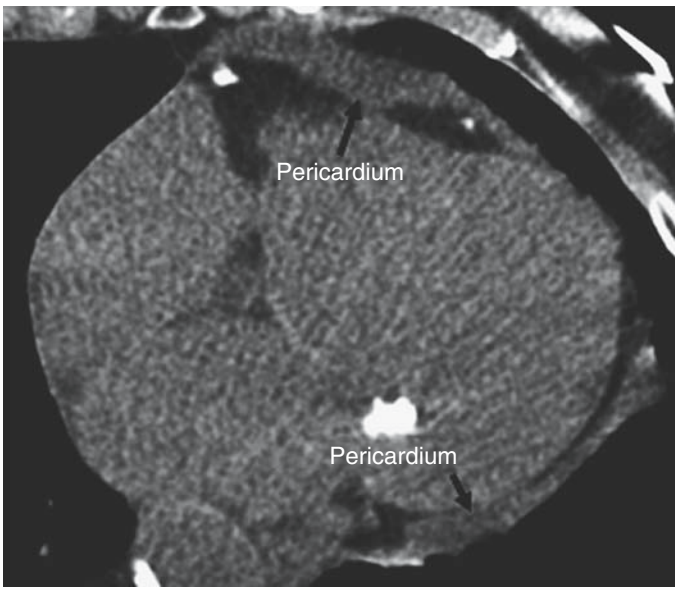

FIGURE 8.16. Severe pericardial thickening of the anterior and posterior sections of the pericardium. Normal pericardium is very thin and barely seen on computed tomographic images. Thickened pericardium is quite visible.

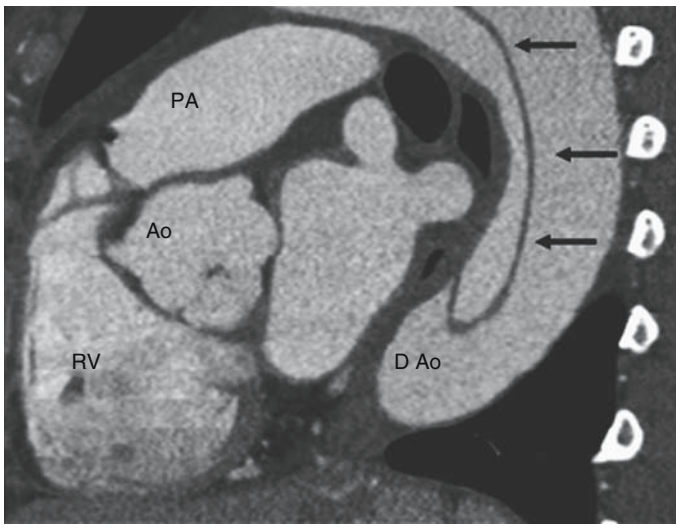

FIGURE 8.17. Large aortic dissection (black arrows), originating in the ascending aorta (Ao) and ending in the descending aorta (D Ao). PA, pulmonary artery; RV, right ventricle.

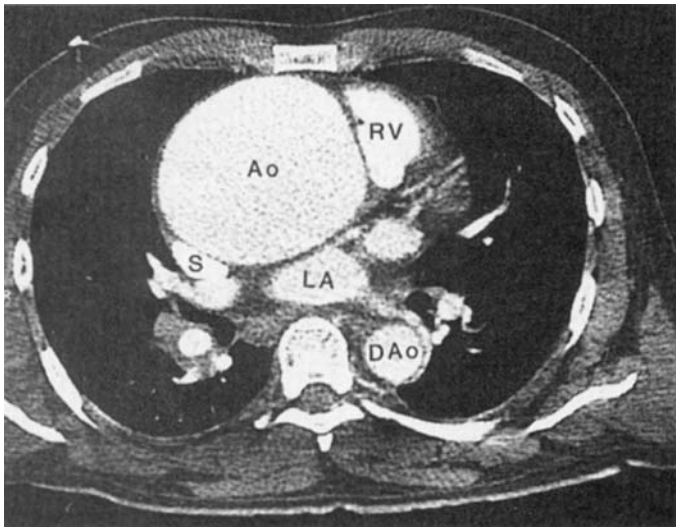

FIGURE 8.18. An 8-cm ascending aortic aneurysm (Ao) is well delineated by ultrafast contrast-enhanced CT. DAo, descending aorta; LA, left atrium; RV, right ventricular outflow tract; S, superior vena cava.

Pulmonary Arteries

Computed tomography can also be utilized to image the pulmonary arteries. Large chronic thrombi, presumably resulting from previous embolization, have been successfully detected by this technique (Fig. 8.19).[141] The cross-sectional view of the main and proximal right and left pulmonary arteries provides clear delineation of the proximal extent of the thrombi, which is essential for successful surgical treatment.[142] Research has indicated that CT may also be a valid method for diagnosis of acute pulmonary embolism.[143,144] Accurate measurement of pulmonary artery size may also be useful in estimating the severity of pulmonary hypertension.[145]

Congenital Heart Disease

Due to advances in surgical management, many patients with congenital heart disease are living into adulthood. The ability to assess the 3D relationships among cardiac, arterial, and venous structures makes CT angiography useful in the diagnosis and follow-up of patients with congenital heart disease in its native and postoperative forms.[146]

Computed tomography angiography is well-suited to the evaluation of congenital abnormalities of the coronary arteries (Fig. 8.20). A rare but important abnormality relating specifically to coronary arteries is anomalous origin of the coronary arteries, with sudden death in young persons during exertion often being the initial presentation.[147] Identification can be difficult by other modalities. Specific anatomies are associated with risk of sudden cardiac death including takeoff of the left coronary artery from the pulmonary trunk, left coronary artery from the right aortic sinus, and right coronary artery from the left aortic sinus.[148] Anomalous coronary arteries can be defined noninvasively by CT angiography,[149,150] as well as by MRI[151] and transesophageal echocardiography.[152]

Considerable experience has been obtained with MRI.[153] Very similar results are now seen with CT high-resolution scanning.[154] The disadvantages of CT are the requirement for injection of contrast medium and exposure to x-ray. Computed tomography offers advantages over MRI, including a single breath-hold to reduce respiratory motion, higher spatial resolution,[155] and reduced slice thickness.[4] An additional advantage of CT is the overall study time of 1 to 2 minutes as compared to 45 to 90 minutes for MR angiography, reducing the time for patients (especially children) to lie perfectly still. As many congenital abnormalities are associated with significant conduction abnormalities or ventricular arrhythmias, many patients with congenital heart disease have pacemakers or implantable cardiac defibrillators in place, contraindicating the use of MRI for imaging. However, MRI may be more applicable to younger patients due to lack

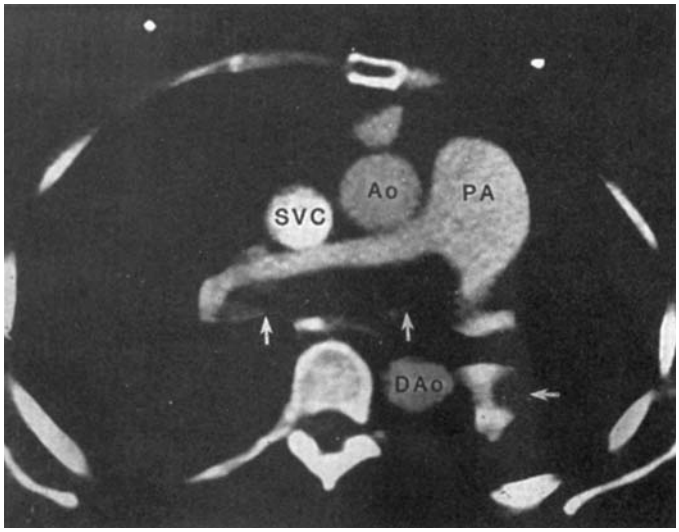

FIGURE 8.19. Large chronic pulmonary embolism (arrows) is shown by contrast-enhanced ultrafast CT to involve the proximal right and left pulmonary arteries. Ao, ascending aorta; DAo, descending aorta; PA, pulmonary artery; SVC, superior vena cava.

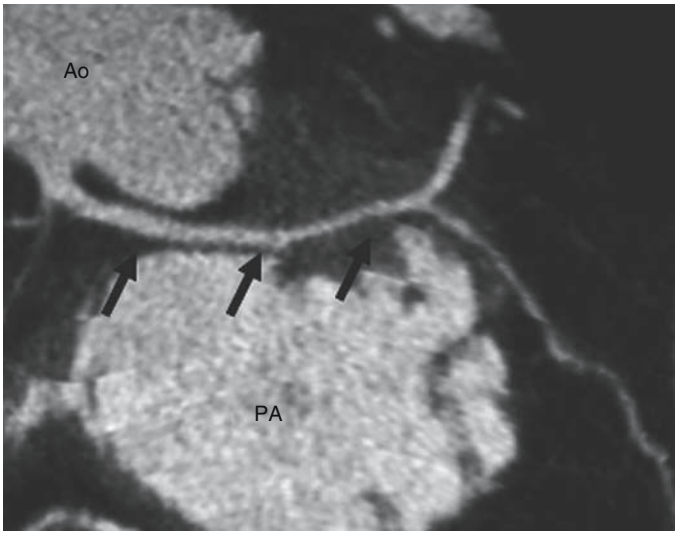

FIGURE 8.20. Anomalous coronary artery with left main coronary artery arising from the right coronary cusp [black arrows depicting the course of the artery between the aorta (Ao) and the pulmonary artery (PA)].

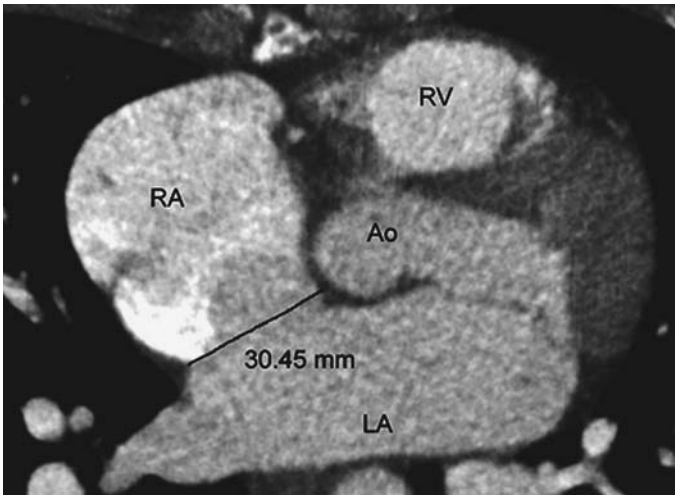

FIGURE 8.21. Secundum atrial septal defect with predominant left to right shunting. Right atrial (RA) enlargement and right ventricular (RV) hypertrophy are present. Ao, ascending aorta; LA, left atrium.

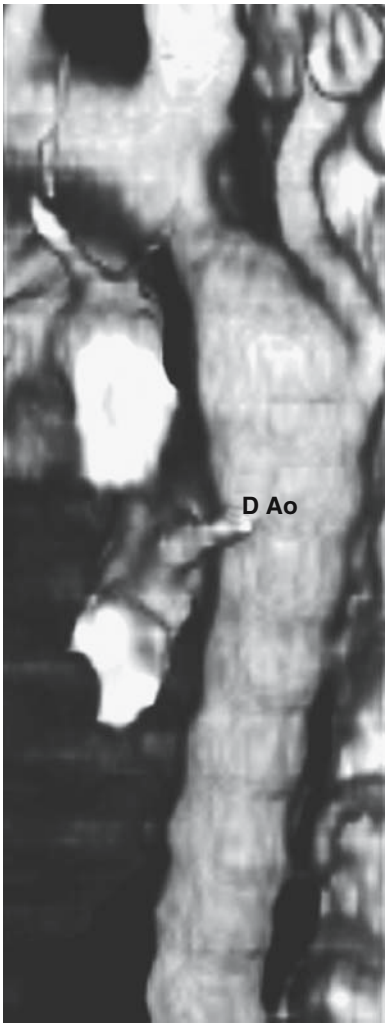

FIGURE 8.22. Coarctation of the aorta. Prominent vertebral artery vessels are noted entering the descending aorta (DAo).

of radiation exposure, but longer study times require a greater need for anesthesia.[156]

Computed tomography imaging can almost always be completed without the need for sedation. The high-resolution images provide excellent detail of the anatomic structure of the cardiac chambers and great vessels. The flow mode can be used to detect and quantitate left-to-right and right-to-left shunts.[157] The cine mode can be used to evaluate RV and LV function, as well as valvular motion. One of the great strengths of cardiac CT is its capacity to study cardiac anatomy, cardiovascular function, and blood flow during a single study period.

A spectrum of cyanotic and acyanotic congenital anomalies can be visualized and characterized by CT angiography (Fig. 8.21).[158] Studies can assess patency of shunts, pulmonary hemodynamics associated with shunts, central pulmonary artery anatomy, anomalous vascular connections, pulmonary vein obstruction, partial anomalous pulmonary venous connections, and other associated thoracic abnormalities such as tracheobronchial abnormalities.[159,160,161,162,163] CT angiography can provide detailed and comprehensive assessment of complex anatomy for surgical planning.[164,165] Congenital abnormalities of the aorta such as coarctation can be easily identified and assessed with 3D imaging (Fig. 8.22).[166]

Electrophysiologic Applications of Cardiac Computed Tomography

Coronary Veins

The same techniques that allow visualization of coronary arteries also visualize the coronary veins (Fig. 8.23). The coronary venous anatomy has become increasingly important as many interventional procedures use the coronary veins to obtain venous access to the left atrium and left ventricle. Computed tomography angiography is effective for visualization of the coronary sinus and its tributaries.[167,168] Computed tomography angiography can provide detailed

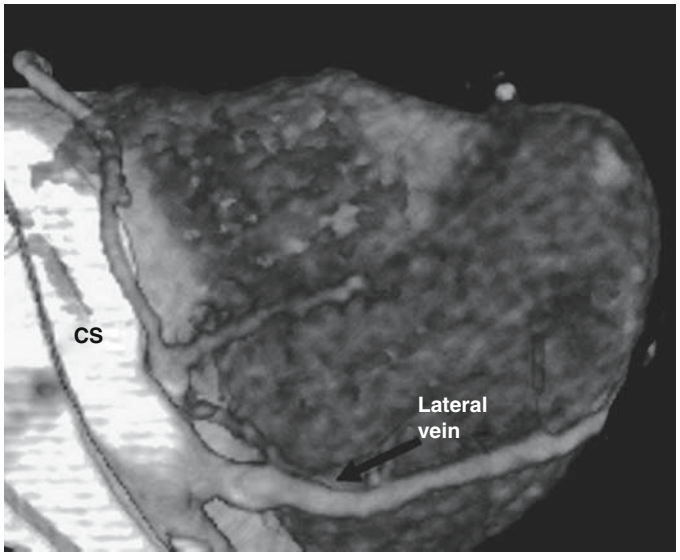

FIGURE 8.23. The coronary venous system is visualized with identification of the coronary sinus (CS) and a large lateral cardiac vein. Distances and diameters can easily be measured.

assessment of the coronary venous anatomy, with coronary sinus dimensions, branch vessel locations, diameters, angulations off the coronary sinus/great cardiac vein, and associated myocardial segment location.[169]

Particular attention has been the focus on coronary venous anatomy with the increasing application of resynchronization therapy. In resynchronization therapy, simultaneous biventricular pacing is performed in patients with dilated or ischemic cardiomyopathy, significant heart failure, and prolonged interventricular conduction in order to "resynchronize" right and left ventricular activation and contraction. The left ventricular component of pacing is provided by a chronic pacing lead placed in a coronary sinus branch vessel, with placement often being challenging due to the need to locate small coronary vein branches for adequate pacing sites. As potential left ventricular pacing sites are defined by an individual patient's coronary venous anatomy, detailed anatomic information could potentially play a role in the approach to resynchronization therapy. Many patients undergoing resynchronization therapy already have devices in place with upgrade to a biventricular system, precluding visualization of anatomy by MRI.

Pulmonary Veins

Characterization of pulmonary venous anatomy is important to catheter-based therapies for atrial fibrillation. Atrial fibrillation has become a major area of research focus due to its increasing incidence in an aging population.[170] Procedural efforts have focused on ablation of the pulmonary vein. Computed tomography angiography and MRI can provide detailed information on pulmonary vein location, variation, size, and complexity, which are difficult to visualize by other techniques; this is important for ablation of pulmonary vein triggers and electrical isolation of pulmonary veins (Fig. 8.24).[171] Endoscopic views of the left atrium can now be achieved through software advances to visualize the complexity of each pulmonary vein os. Additionally, follow-up of patients for such complications as pulmonary vein stenosis is extremely important.[172] The incidence and time course of pulmonary vein stenosis requires further definition, through serial evaluation of pulmonary vein structure.

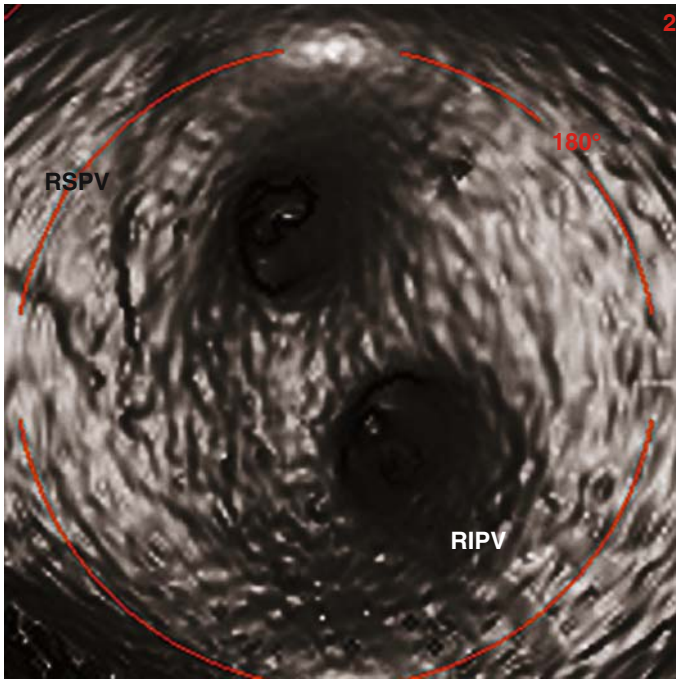

FIGURE 8.24. Endoscopic view of the right superior and inferior pulmonary veins (RSPV and RIPV).

Summary

Computed tomography coronary artery calcium assessment and CT coronary angiography using EBCT or MDCT are technologies that can provide risk stratification for future cardiac events and definition of patient populations requiring aggressive risk factor modification or interventional therapy for CAD. Computed tomography angiography is a robust technology that can identify a spectrum of cardiovascular disease processes and facilitation of invasive cardiac procedures. Further advances in technology and methodology will broaden the research applications for the understanding of cardiovascular pathophysiology and clinical applications for diagnosis and treatment of cardiovascular disease. The availability of many other imaging modalities and the relatively high cost of CT scanners and limited or lack of reimbursement have slowed its adoption for diagnosis by cardiologists, radiologists, and primary caregivers. However, the technology offers some truly unique capabilities, with unmatched prognostic capabilities for cardiac events and noninvasive imaging of the coronary arteries and veins, and clinicians are increasingly employing this imaging technique. Cardiac CT is considered by some to be the gold standard in evaluating congenital heart disease, pulmonary vein anatomy, and coronary venous anatomy. Further experience and utilization will undoubtedly increase the interest and knowledge of this multifaceted tool.

References

1. Agatston AS, Janowitz WR, Hildner FJ, Zusmer NR, Viamonte M Jr, Detrano R. Quantification of coronary artery calcium using ultrafast computed tomography. J Am Coll Cardiol 1990;15:827–832.
2. Lu B, Mao SS, Zhuang N, et al. Coronary artery motion during the cardiac cycle and optimal ECG triggering for coronary artery imaging. Invest Radiol 2001;36:250–256.
3. Becker CR, Kleffel T, Crispin A, et al. Coronary artery calcium measurement: agreement of multirow detector and electron beam CT. AJR 2001;176:1295–1298.
4. Budoff MJ, Achenbach S, Duerinckx A. Clinical utility of computed tomography and magnetic resonance techniques for noninvasive coronary angiography. J Am Coll Cardiol 2003; 42:1867–1878.
5. Nasir K, Budoff MJ, Post WS, et al. Electron Beam CT vs. Helical CT scans of coronary arteries: current utility and future directions. Am Heart J 2003:146:949–977.
6. Hunold P, Vogt FM, Schmermund A, et al. Radiation exposure during cardiac CT: effective doses at multi-detector row CT and electron-beam CT. Radiology 2003;226:145–152.
7. Manning WJ, Li W, Edelman RR. A preliminary report comparing magnetic resonance imaging with conventional angiography. N Engl J Med 1993;328:828–832.
8. Pennell DJ, Keegan J, Firmin DN, Gatehouse PD, Underwood SR, Longmore DB. Magnetic resonance imaging of coronary arteries: technique and preliminary results. Br Heart J 1993; 70:315–326.

9. Paschal CB, Haache EM, Adler LP. Coronary arteries: three-dimensional MR imaging of the coronary arteries: preliminary clinical experience. J MRI 1993;3:491–501.
10. Duerinckx AJ, Urman MK. Two dimensional coronary MR angiography: analysis of initial clinical results. Radiology 1994;193:731–738.
11. Duerinckx AJ, Urman MK, Atkinson DJ, Simonetti OP, Sinha U, Lewis B. Limitations of MR coronary angiography. J MRI 19943;4:81.
12. Duerinckx AJ, Atkinson DP, Mintorovitch J, Simonetti OP, Vrman MK. Two-dimensional coronary MRA: limitations and artifacts. Eur Radiol 1996;6:312–325.
13. Kim WY, Danias PG, Stuber M, et al. Coronary magnetic resonance angiography for the detection of coronary stenoses. N Engl J Med 2001;345:1863–1869.
14. Chernoff DM, Ritchie CJ, Higgins CB. Evaluation of electron beam CT coronary angiography in healthy subjects. AJR 1997; 169:93–99.
15. Bostrom K, Watson KE, Horn S, Wortham C, Herman IM, Demer LL. Bone morphogenetic protein expression in human atherosclerotic lesions. J Clin Invest 1993;91:1800–1809.
16. Eggen DA, Strong JP, McGill HC Jr. Coronary calcification. Relationship to clinically significant coronary lesions and race, sex, and topographic distribution. Circulation 1965;32: 948–955.
17. Mautner SL, Mautner GC, Froehlich J, et al. Coronary artery disease: prediction with in vitro electron beam CT. Radiology 1994;192:625–630.
18. Schmermund A, Baumgart D, Gorge G, et al. Coronary artery calcium in acute coronary syndromes: a comparative study of electron-beam computed tomography, coronary angiography, and intracoronary ultrasound in survivors of acute myocardial infarction and unstable angina. Circulation 1997;96:1461–1469.
19. Mintz GS, Pichard AD, Popma JJ, et al. Determinants and correlates of target lesion calcium in coronary artery disease: a clinical, angiographic and intravascular ultrasound study. J Am Coll Cardiol 1997;29:268–274.
20. Rumberger JA, Simons DB, Fitzpatrick LA, Sheedy PF, Schwartz RS. Coronary artery calcium area by electron-beam computed tomography and coronary atherosclerotic plaque area. A histopathologic correlative study. Circulation 1995;92:2157–2162.
21. Callister TQ, Raggi P, Cooil B, Lippolis NJ, Russo DJ. Effect of HMG-CoA reductase inhibitors on coronary artery disease as assessed by electron beam computed tomography. N Engl J Med 1998;339:1972–1978.
22. Budoff MJ, Mao S, Lu B, et al. Ability of calibration phantom to reduce the interscan variability in electron beam computed tomography. J Comput Assist Tomogr 2002;26(6):886–891.
23. Wong ND, Budoff MJ, Pio J, Detrano RC. Coronary calcium and cardiovascular event risk: evaluation by age- and sex-specific quartiles. Am Heart J 2002;143:456–459.
24. Achenbach S, Ropers D, Mohlenkamp S, et al. Variability of repeated coronary artery calcium measurements by electron beam tomography. Am J Cardiol 2001;87:210–213.
25. Mao S, Bakhsheshi H, Lu B, Liu SC, Oudiz RJ, Budoff MJ. Effect of electrocardiogram triggering on reproducibility of coronary artery calcium scoring. Radiology 2001;220:707–711.
26. Daniell AL, Wong ND, Friedman JD, et al. Reproducibility of coronary calcium measurements from multidetector computed tomography. J Am Coll Cardiol 2003;41(suppl A):456–457.
27. Budoff MJ, Lane KL, Bakhsheshi H, et al. Rates of progression of coronary calcification by electron beam computed tomography. Am J Cardiol 2000;86(1):8–11.
28. Raggi P, Cooil B, Shaw L, et al. Progression of coronary calcification on serial electron beam tomography scanning is greater in patients with future myocardial infarction. Am J Cardiol 2003;92:827–829.
29. Raggi P, Callister TQ, Shaw LJ. Progression of coronary artery calcium and risk of first myocardial infarction in patients receiving cholesterol-lowering therapy. Arterioscler Thromb Vasc Biol 2004;24(7):1272–1277.
30. Baumgart D, Schmermund A, Goerge G, et al. Comparison of electron beam computed tomography with intracoronary ultrasound and coronary angiography for detection of coronary atherosclerosis. J Am Coll Cardiol 1997;30:57–64.
31. Mautner GC, Mautner SL, Froehlich J, et al. Coronary artery calcification: assessment with electron beam CT and histomorphometric correlation. Radiology 1994;192:619–623.
32. Budoff MJ, Georgiou D, Brody A, et al. Ultrafast computed tomography as a diagnostic modality in the detection of coronary artery disease: a multicenter study. Circulation 1996; 93:898–904.
33. Haberl R, Becker A, Leber A, et al. Correlation of coronary calcification and angiographically documented stenoses in patients with suspected coronary artery disease: results of 1,764 patients. J Am Coll Cardiol 2001;37:451–457.
34. Guerci A, Spadaro L, Goodman KG, et al. Comparison of electron beam computed tomography scanning and conventional risk factor assessment for the prediction of angiographic coronary artery disease. J Am Coll Cardiol 1998;32: 673–677.
35. Schmermund A, Erbel R. Unstable coronary plaque and its relation to coronary calcium. Circulation 2001;104:1682–1687.
36. Rumberger JA, Sheedy PF, Breen JF, Schwartz RS. Electron beam computed tomographic coronary calcium score cutpoints and severity of associated angiographic lumen stenosis. J Am Coll Cardiol 1997;29:1542–1548.
37. Budoff MJ, Diamond GA, Raggi P, et al. Continuous probabilistic prediction of angiographically significant coronary artery disease using electron beam tomography. Circulation 2002; 105:1791–1796.
38. Shavelle DM, Budoff MJ, LaMont DH, Shavelle RM, Kennedy JM, Brundage BH. Exercise testing and electron beam computed tomography in the evaluation of coronary artery disease. J Am Coll Cardiol 2000;36:32–38.
39. Kajinami K, Seki H, Takekoshi N, Mabuchi H. Noninvasive prediction of coronary atherosclerosis by quantification of coronary artery calcification using electron beam computed tomography: comparison with electrocardiographic and thallium exercise stress test results. J Am Coll Cardiol 1995;26: 1209–1221.
40. Lamont DH, Budoff MJ, Shavelle DM, Shavelle R, Brundage BH, Hagar JM. Coronary calcium scanning adds incremental value to patients with positive stress tests. Am Heart J 2002;143(5): 861–867.
41. Kannel WB, Schatzkin A. Sudden death: lessons from subsets in population studies. J Am Coll Cardiol 1985;5:141B–149B.
42. Raggi P. Coronary calcium screening to improve risk stratification in primary prevention. J La State Med Soc 2002;154: 314–318.
43. Little WC, Constantinescu M, Applegate RJ, et al. Can coronary angiography predict the site of a subsequent myocardial infarction in patients with mild-to-moderate coronary artery disease? Circulation 1988;78:1157–1166.
44. Giroud D, Li JM, Urban P, Meier B, Rutishauer W. Relation of the site of acute myocardial infarction to the most severe coronary arterial stenosis at prior angiography. Am J Cardiol 1992;69:729–732.
45. Roberts WC, Jones AA. Quantitation of coronary arterial narrowing at necropsy in sudden coronary death: analysis of 31 patients and comparison with 25 control subjects. Am J Cardiol 1979;44:39–45.

46. Margolis JR, Chen JT, Kong Y, Peter RH, Behar VS, Kisslo JA. The diagnostic and prognostic significance of coronary artery calcification. A report of 800 cases. Radiology 1980;137: 609–616.
47. Georgiou D, Budoff MJ, Kaufer E, Kennedy JM, Lu B, Brundage BH. Screening patients with chest pain in the emergency department using electron beam tomography: a follow-up study. J Am Coll Cardiol 2001;38:105–110.
48. Detrano R, Hsiai T, Wang S, et al. Prognostic value of coronary calcification and angiographic stenoses in patients undergoing coronary angiography. J Am Coll Cardiol 1996;27:285–290.
49. Kennedy J, Shavelle R, Wang S, Budoff M, Detrano RC. Coronary calcium and standard risk factors in symptomatic patients referred for coronary angiography. Am Heart J 1998;135: 696–702.
50. Keelan PC, Bielak LF, Ashai K, et al. Long-term prognostic value of coronary calcification detected by electron-beam computed tomography in patients undergoing coronary angiography. Circulation 2001;104:412–417.
51. Shepherd J, Cobbe SM, Ford I, et al. Prevention of coronary heart disease with pravastatin in men with hypercholesterolemia. West of Scotland Coronary Prevention Study Group. N Engl J Med 1995;333:1301–1307.
52. Arad Y, Spadaro LA, Goodman K, Newstein D, Guerci AD. Prediction of coronary events with electron beam computed tomography. J Am Coll Cardiol 2000;36:1253–1260.
53. Wong ND, Hsu JC, Detrano RC, Diamond G, Eisenberg H, Gardin JM. Coronary artery calcium evaluation by electron beam computed tomography and its relation to new cardiovascular events. Am J Cardiol 2000;86:495–498.
54. Greenland P, LaBree L, Azen SP, Doherty TM, Detrano RC. Coronary artery calcium score combined with Framingham score for risk prediction in asymptomatic individuals. JAMA 2004;291:210–215.
55. Raggi P, Cooil B, Callister TQ. Use of electron beam tomography data to develop models for prediction of hard coronary events. Am Heart J 2001;141:375–382.
56. Kondos GT, Hoff JA, Sevrukov A, et al. Electron-beam tomography coronary artery calcium and cardiac events: a 37-month follow-up of 5635 initially asymptomatic low- to intermediate-risk adults. Circulation 2003;107:2571–2576.
57. Arad Y, Roth M, Newstein D, Guerci AD. Coronary calcification, coronary risk factors, and atherosclerotic cardiovascular disease events. The St. Francis Heart Study. J Am Coll Cardiol 2005;46:158–165.
58. Shaw LJ, Raggi P, Schisterman E, et al. Prognostic value of cardiac risk factors and coronary artery calcium screening for all-cause mortality. Radiology 2003;28:826–833.
59. Grundy SM. Coronary plaque as a replacement for age as a risk factor in global risk assessment. Am J Cardiol 2001;88: 8E–11E.
60. O'Rourke RA, Brundage BH, Froelicher VF, et al. American College of Cardiology/American Heart Association Expert Consensus Document on electron-beam computed tomography for the diagnosis and prognosis of coronary artery disease. J Am Coll Cardiol 2000;36:326–340.
61. Executive Summary of The Third Report of The National Cholesterol Education Program (NCEP) Expert Panel on Detection, Evaluation, and Treatment of High Blood Cholesterol in Adults (Adult Treatment Panel III). JAMA 2001;285:2486–2497.
62. Smith SC Jr, Amsterdam E, Balady GJ, et al. Prevention Conference V: Beyond secondary prevention: identifying the high-risk patient for primary prevention: tests for silent and inducible ischemia: Writing Group II. Circulation 2000;101:E12–16.
63. Mosca L, Appel LJ, Benjamin EJ, et al. Evidence-based guidelines for cardiovascular disease prevention in women. Circulation 2004;109:672–693.
64. Rumberger JA, Behrenbeck T, Breen JF, Sheedy PF 2nd. Coronary calcification by electron beam computed tomography and obstructive coronary artery disease: a model for costs and effectiveness of diagnosis as compared with conventional cardiac testing methods. J Am Coll Cardiol 1999;33:453–462.
65. Nasir K, Redberg RF, Budoff MJ, Hui E, Post WS, Blumenthal RS. Utility of stress testing and coronary calcification measurement for detection of coronary artery disease in women. Arch Intern Med 2004;164:1610–1620.
66. Budoff MJ, Shakooh S, Shavelle RM, Kim HT, French WJ. Electron beam tomography and angiography: sex differences. Am Heart J 2002;143(5):877–882.
67. Laudon DA, Vukov LF, Breen JF, Rumberger JA, Wollan PC, Sheedy PF 2nd. Use of electron-beam computed tomography in the evaluation of chest pain patients in the emergency department. Ann Emerg Med 1999;33:15–21.
68. McLaughlin VV, Balogh T, Rich S. Utility of electron beam computed tomography to stratify patients presenting to the emergency room with chest pain. Am J Cardiol 1999;84: 327–328.
69. Budoff MJ, Shavelle DM, Lamont DH, et al. Usefulness of electron beam computed tomography scanning for distinguishing ischemic from nonischemic cardiomyopathy. J Am Coll Cardiol 1998;32:1173–1178.
70. Mieres JH, Shaw LJ, Arai A, et al. The role of non-invasive testing in the clinical evaluation of women with suspected coronary artery disease: american heart association consensus statement. Circulation 2005;111:682–696.
71. Greenland P, Abrams J, Aurigemma GP, et al. Prevention Conference V: Beyond secondary prevention: identifying the high-risk patient for primary prevention: noninvasive tests of atherosclerotic burden: Writing Group III. Circulation 2000;101(1):E16–E22.
72. Taylor AJ, Merz CN, Udelson JE. 34th Bethesda Conference: Executive summary—can atherosclerosis imaging techniques improve the detection of patients at risk for ischemic heart disease? J Am Coll Cardiol 2003;41(11):1860–1862.
73. Grundy SM, Cleeman JI, Merz CN, et al. Implications of recent clinical trials for the National Cholesterol Education Program Adult Treatment Panel III guidelines. Circulation 2004; 110(2):227–239.
74. Nakanishi T, Ito K, Imazu M, Yamakido M. Evaluation of coronary artery stenoses using electron-beam CT and multiplanar reformation. J Comput Assist Tomogr 1997;21:121–127.
75. Achenbach S, Moshage W, Ropers D, Bachmann K. Curved multiplanar reconstructions for the evaluation of contrast-enhanced electron beam CT of the coronary arteries. AJR 1998;170:895–899.
76. Budoff MJ, Oudiz RJ, Zalace CP, et al. Intravenous three dimensional coronary angiography using contrast enhanced electron beam computed tomography. Am J Cardiol 1999;83: 840–845.
77. Reddy GP, Chernoff DM, Adams JR, Higgins CB. Coronary artery stenoses: assessment with contrast-enhanced electron-beam CT and axial reconstructions. Radiology 1998;208: 167–172.
78. Achenbach S, Moshage W, Ropers D, Nossen J, Daniel WG. Value of electron-beam computed tomography for the noninvasive detection of high-grade coronary artery stenoses and occlusions. N Engl J Med 1998;339:1964–1971.
79. Chernoff DM, Ritchie CJ, Higgins CB. Evaluation of electron beam CT coronary angiography in healthy subjects. AJR 1997; 169:93–99.
80. Moshage WE, Achenbach S, Seese B, Bachmann K, Kirchgeorg M. Coronary artery stenoses: three-dimensional imaging with electrocardiographically triggered, contrast agent-enhanced, electron-beam CT. Radiology 1995;196:707–714.

81. Achenbach S, Moshage W, Ropers D, Bachmann K. Comparison of vessel diameters in electron beam tomography and quantitative coronary angiography. Int J Card Imaging 1998;14:1–7; discussion 9.
82. Lu B, Mao SS, Zhuang N, et al. Coronary artery motion during the cardiac cycle and optimal ECG triggering for coronary artery imaging. Invest Radiol 2001;36:250–256.
83. Mao S, Oudiz RJ, Bakhsheshi H, Liu SCK, Budoff MJ. Coronary artery motion and coronary artery imaging. J Comput Assist Tomogr 2000;24:253–258.
84. Lu B, Shavelle DM, Mao SS, et al. Improved accuracy of noninvasive electron beam coronary angiography. Invest Radiol 2004;39(2):73–79.
85. Budoff MJ, Lu B, Shinbane JS, et al. Methodology for improved detection of coronary stenoses with computed tomographic angiography. Am Heart J 2004;148(6):1085–1090.
86. Budoff MJ, Shinbane JS, Oudiz RJ, et al. Comparison of coronary artery calcium screening image quality between C-150 and e-speed electron beam scanners. Acad Radiol 2005;12(3): 309–312.
87. Rasouli ML, Shavelle DM, French WJ, McKay CR, Budoff MJ. Assessment of coronary plaque morphology by contrast-enhanced computed tomographic angiography: comparison with intravascular ultrasound. Coron Artery Dis 2006;17: 359–364.
88. Achenbach S, Giesler T, Ropers D, et al. Detection of coronary artery stenoses by contrast-enhanced, retrospectively electrocardiographically-gated, multislice spiral computed tomography. Circulation 2001;103:2535–2538.
89. Giesler T, Baum U, Ropers D, et al. Noninvasive visualization of coronary arteries using contrast-enhanced multidetector CT: influence of heart rate on image quality and stenosis detection. AJR 2002;179:911–916.
90. Nieman K, Rensing BJ, van Geuns RJ, et al. Non-invasive coronary angiography with multislice spiral computed tomography: impact of heart rate. Heart 2002;88:470–474.
91. Budoff MJ. Non-invasive coronary angiography using computed tomography. Expert Rev Cardiovasc Ther 2005;3:123–132.
92. Hoffmann U, Moselewski F, Cury RC, et al. Predictive value of 16–slice multidetector spiral computed tomography to detect significant obstructive coronary artery disease in patients at high risk for coronary artery disease: patient versus segment-based analysis. Circulation 2004;110(17):2638–2643. E-pub 2004; October 18.
93. Ropers D, Baum U, Pohle K, et al. Detection of coronary artery stenoses with thin-slice multi-detector row spiral computed tomography and multiplanar reconstruction. Circulation 2003; 107:664–666.
94. Nieman K, Cademartiri F, Lemos PA, Raaijmakers R, Pattynama PM, de Feyter PJ. Reliable noninvasive coronary angiography with fast submillimeter multislice spiral computed tomography. Circulation 2002;106:2051–2054.
95. Bateman TM, Gray RJ, Whiting JS, Matloff JM, Berman DS, Forrester JS. Cine computed tomographic evaluation of aortocoronary bypass graft patency. J Am Coll Cardiol 1986;8:693–698.
96. Achenbach S, Moshage W, Ropers D, Nossen J, Bachmann K. Noninvasive, three-dimensional visualization of coronary artery bypass grafts by electron beam tomography. Am J Cardiol 1997;79:856–861.
97. Ha JW, Cho SY, Shim WH, et al. Noninvasive evaluation of coronary artery bypass graft patency using three-dimensional angiography obtained with contrast-enhanced electron beam CT. AJR 1999;172:1055–1059.
98. Schlosser T, Konorza T, Hunold P, Kuhl H, Schmermund A, Barkhausen J. Noninvasive visualization of coronary artery bypass grafts using 16–detector row computed tomography. J Am Coll Cardiol 2004;44(6):1224–1229.
99. Achenbach S, Moshage W, Bachmann K. Detection of high-grade restenosis after PTCA using contrast-enhanced electron beam CT. Circulation 1997;96:2785–2788.
100. Pump H, Moehlenkamp S, Sehnert C, et al. Electron-beam CT in the noninvasive assessment of coronary stent patency. Acad Radiol 1998;5:858–862.
101. Lu B, Dai R, Bai H, et al. Detection and analysis of intracoronary artery stent after PTCA using contrast-enhanced three-dimensional electron beam tomography. J Invasive Cardiol 2000;12:1–6.
102. Nissen SE, Gurley JC, Grines CL, et al. Intravascular ultrasound assessment of lumen size and wall morphology in normal subjects and patients with coronary artery disease. Circulation 1991;84:1087–1099.
103. Mintz GS, Painter JA, Pichard AD, et al. Atherosclerosis in angiographically "normal" coronary artery reference segments: an intravascular ultrasound study with clinical correlations. J Am Coll Cardiol 1995;25:1479–1485.
104. Schmermund A, Baumgart D, Adamzik M, et al. Comparison of electron-beam computed tomography and intracoronary ultrasound in detecting calcified and noncalcified plaques in patients with acute coronary syndromes and no or minimal to moderate angiographic coronary artery disease. Am J Cardiol 1998;81:141–146.
105. Achenbach S, Moselewski F, Ropers D, et al. Detection of calcified and noncalcified coronary atherosclerotic plaque by contrast-enhanced, submillimeter multidetector spiral computed tomography: a segment-based comparison with intravascular ultrasound. Circulation 2004;109:14–17.
106. Achenbach S, Giesler T, Ropers D, et al. Detection of coronary artery stenoses by contrast-enhanced, retrospectively electrocardiographically-gated, multislice spiral computed tomography. Circulation 2001;103:2535–2538.
107. Knollmann FD, Hidajat N, Felix R. CTA of the coronary arteries: comparison of radiation exposure with EBCT and multislice detector CT. Radiology 2000;217(P):364.
108. International Commission on Radiological Protection. Recommendation of the ICRP. ICRP Publication 60. Oxford: Pergamon Press, 1990.
109. Morin RL, Gerber TC, McCollough CH. Radiation dose in computed tomography of the heart. Circulation 2003;107: 917–922.
110. Flohr TG, Schoepf UJ, Kuettner A, et al. Advances in cardiac imaging with 16–section CT systems. Acad Radiol 2003;10(4): 386–401.
111. Trabold T, Buchgeister M, Kuttner A, et al. Estimation of radiation exposure in 16–detector row computed tomography of the heart with retrospective ECG-gating. Rofo 2003;175: 1051–1055.
112. Achenbach S, Moshage W, Ropers D, Bachmann K. Curved multiplanar reconstructions for the evaluation of contrast-enhanced electron beam CT of the coronary arteries. AJR 1998;170:895–899.
113. Ropers D, Moshage W, Daniel WG, Jessl J, Gottwik M, Achenbach S. Visualization of coronary artery anomalies and their anatomic course by contrast-enhanced electron beam tomography and three-dimensional reconstruction. Am J Cardiol 2001;87:193–197.
114. Baik HK, Budoff MJ, Lane KL, Bakhsheshi H, Brundage BH. Accurate measures of left ventricular ejection fraction using electron beam tomography: a comparison with radionuclide angiography, and cine angiography. Int J Card Imaging 2000; 16:391–398.
115. Rich S, Chomka EV, Stagl R, Shanes JG, Kondos GT, Brundage BH. Determination of left ventricular ejection fraction using ultrafast computed tomography. Am Heart J 1986;112:392–396.

116. Rumberger JA, Behrenbeck T, Bell MR, et al. Determination of ventricular ejection fraction: a comparison of available imaging methods. The Cardiovascular Imaging Working Group. Mayo Clin Proc 1997;72:860–870.
117. Reiter SJ, Rumberger JA, Feiring AJ, Stanford W, Marcus ML. Precision of measurements of right and left ventricular volume by cine computed tomography. Circulation 1986;74:890–900.
118. Schmermund A, Rensing BJ, Sheedy PF, Rumberger JA. Reproducibility of right and left ventricular volume measurements by electron-beam CT in patients with congestive heart failure. Int J Card Imaging 1998;14:201–209.
119. Feiring AJ, Rumberger JA, Reiter SJ, et al. Determination of left ventricular mass in dogs with rapid-acquisition cardiac computed tomographic scanning. Circulation 1985;72:1355–1364.
120. Mousseaux E, Beygui F, Fornes P, et al. Determination of left ventricular mass with electron beam computed tomography in deformed, hypertrophic human hearts. Eur Heart J 1994; 15:832–841.
121. Feiring AJ, Rumberger JA. Ultrafast computed tomography analysis of regional radius-to-wall thickness ratios in normal and volume-overloaded human left ventricle. Circulation 1992; 85:1423–1432.
122. Gerber TC, Schmermund A, Reed JE, et al. Use of a new myocardial centroid for measurement of regional myocardial dysfunction by electron beam computed tomography: comparison with technetium-99m sestamibi infarct size quantification. Invest Radiol 2001;36:193–203.
123. Rumberger JA, Weiss RM, Feiring AJ, et al. Patterns of regional diastolic function in the normal human left ventricle: an ultrafast computed tomographic study. J Am Coll Cardiol 1989; 14:119.
124. Gerber TC, Behrenbeck T, Allison T, Mullan BP, Rumberger JA, Gibbons RJ. Comparison of measurement of left ventricular ejection fraction by Tc-99m sestamibi first-pass angiography with electron beam computed tomography in patients with anterior wall acute myocardial infarction. Am J Cardiol 1999;83:1022–1026.
125. Budoff MJ, Gillespie R, Georgiou D, et al. Comparison of exercise electron beam computed tomography and sestamibi in the evaluation of coronary artery disease. Am J Cardiol 1998;81:682–687.
126. Hattori Y, Imazu M, Yamabe T, Yamakido M, Nakanishi T, Ito K. Comparative study of dobutamine stress electron-beam computed tomography and exercise thallium scintigraphy in the diagnosis of patients with suspected coronary artery disease. Jpn Circ J 1998;62(2):83–90.
127. Maron MS, Olivotto I, Betocchi S, et al. Effect of left ventricular outflow tract obstruction on clinical outcome in hypertrophic cardiomyopathy. N Engl J Med 2003;348:295–303.
128. Klues HG, Schiffers A, Maron BJ. Phenotypic spectrum and patterns of left ventricular hypertrophy in hypertrophic cardiomyopathy: morphologic observations and significance as assessed by two-dimensional echocardiography in 600 patients. J Am Coll Cardiol 1995;26:1699–1708.
129. Juergens KU, Wessling J, Fallenberg EM, Monnig G, Wichter T, Fischbach R. Multislice cardiac spiral CT evaluation of atypical hypertrophic cardiomyopathy with a calcified left ventricular thrombus. J Comput Assist Tomogr 2000;24:688–690.
130. Funabashi N, Yoshida K, Komuro I. Thinned myocardial fibrosis with thrombus in the dilated form of hypertrophic cardiomyopathy demonstrated by multislice computed tomography. Heart 2003;89:858.
131. Schulz-Menger J, Strohm O, Waigand J, Uhlich F, Dietz R, Friedrich MG. The value of magnetic resonance imaging of the left ventricular outflow tract in patients with hypertrophic obstructive cardiomyopathy after septal artery embolization. Circulation 2000;101:1764–1766.
132. Dery R, Lipton MJ, Garrett JS, Abbott J, Higgins CB, Schienman MM. Cine-computed tomography of arrhythmogenic right ventricular dysplasia. J Comput Assist Tomogr 1986;10:120–123.
133. Corrado D, Thiene G, Nava A, Rossi L, Pennelli N. Sudden death in young competitive athletes: clinicopathologic correlations in 22 cases. Am J Med 1990;89:588–596.
134. di Cesare E. MRI assessment of right ventricular dysplasia. Eur Radiol 2003;13:1387–1393.
135. Hamada S, Takamiya M, Ohe T, Ueda H. Arrhythmogenic right ventricular dysplasia: evaluation with electron-beam CT. Radiology 1993;187:723–727.
136. Tada H, Shimizu W, Ohe T, et al. Usefulness of electron-beam computed tomography in arrhythmogenic right ventricular dysplasia. Relationship to electrophysiological abnormalities and left ventricular involvement. Circulation 1996;94:437–444.
137. Lu B, Dai RP, Jing BL, et al. Electron beam tomography with three-dimensional reconstruction in the diagnosis of aortic diseases. J Cardiovasc Surg (Torino) 2000;41:659–668.
138. Stanford W. Computed tomography in the diagnosis of pericardial disease. In: Brundage BH, ed. Comparative Cardiac Imaging. Rockville, MD: Aspen, 1990:451–457.
139. Stanford W, Rooholamini SA, Galvin JR. Assessment of intracardiac masses and extracardiac abnormalities by ultrafast computed tomography. In: Marcus ML, Schelbert HR, Skorton DJ Wolf GL, eds. Cardiac Imaging. Philadelphia: WB Saunders, 1991:703.
140. Rooholamini SA, Stanford W. Ultrafast computed tomography in the diagnosis of aortic aneurysms and dissections. In: Stanford W, Rumberger J, eds. Ultrafast Computed Tomography in Cardiac Imaging: Principles and Practice. Mount Kisco, NY: Futura, 1992:287–310.
141. Rich S, Levitsky S, Brundage BH. Pulmonary hypertension from chronic pulmonary thromboembolism. Ann Intern Med 1989;108:425.
142. Moser KM, Auger WR, Fedullo PF. Chronic major-vessel thromboembolic pulmonary hypertension. Circulation 1990;81:1735.
143. Galvin JR, Gingrich RD, Hoffman E, Kao SC, Stern EJ, Stanford W. Ultrafast computed tomography of the chest. Radiol Clin North Am 1994;32:775–793.
144. Stanford W, Reiners TJ, Thompson BH, et al. Contrast enhanced thin slice ultrafast computed tomography for the detection of small pulmonary emboli in the pig. Invest Radiol 1994;29: 184–187.
145. Kuriyama K, Gamsu G, Stern RG, et al. CT determined pulmonary artery diameters in predicting pulmonary hypertension. Invest Radiol 1984;19:16.
146. Farmer DW, Lipton MJ, Webb WR, Ringertz H, Higgins CB. Computed tomography in congenital heart disease. J Comput Assist Tomogr 1984;8:677–687.
147. Maron BJ, Shirani J, Poliac LC, Mathenge R, Roberts WC, Mueller FO. Sudden death in young competitive athletes. Clinical, demographic, and pathological profiles. JAMA 1996; 276:199–204.
148. Frescura C, Basso C, Thiene G, et al. Anomalous origin of coronary arteries and risk of sudden death: a study based on an autopsy population of congenital heart disease. Hum Pathol 1998;29:689–695.
149. Li W, Ferrett C, Henein M. Images in cardiovascular medicine. Anomalous coronary arteries by electron beam angiography. Circulation 2003;107:2630.
150. Ropers D, Moshage W, Daniel WG, Jessl J, Gottwik M, Achenbach S. Visualization of coronary artery anomalies and their anatomic course by contrast-enhanced electron beam tomography and three-dimensional reconstruction. Am J Cardiol 2001;87:193–197.

151. Post JC, van Rossum AC, Bronzwaer JG, et al. Magnetic resonance angiography of anomalous coronary arteries. A new gold standard for delineating the proximal course? Circulation 1995;92:3163–3171.
152. Fernandes F, Alam M, Smith S, Khaja F. The role of transesophageal echocardiography in identifying anomalous coronary arteries. Circulation 1993;88:2532–2540.
153. Kersting-Sommerhoff B, Higgins CB: Magnetic resonance of congenital heart disease. In: Brundage BH, ed. Comparative Cardiac Imaging. Rockville, MD: Aspen, 1990:493–502.
154. AboulHosn J, Shavelle DM, Budoff M, Criley JM. Electron beam angiography in adults with congenital heart disease. Cathet Cardiovasc Intervent 2004;27(12):702.
155. Duerinckx AJ, Urman MK, Atkinson DJ, Simonetti OP, Sinha U, Lewis B. Limitations of MR coronary angiography. J MRI 1994;4:81.
156. Kawano T, Ishii M, Takagi J, et al. Three-dimensional helical computed tomographic angiography in neonates and infants with complex congenital heart disease. Am Heart J 2000; 139:654–660.
157. Garrett J, Jaschke W, Aherne T, et al. Quantitation of intracardiac shunts by cine-CT. J Comput Assist Tomogr 1988;12:82.
158. Choi BW, Park YH, Choi JY, et al. Using electron beam CT to evaluate conotruncal anomalies in pediatric and adult patients. AJR 2001;177:1045–1049.
159. Chen SJ, Li YW, Wang JK, et al. Three-dimensional reconstruction of abnormal ventriculoarterial relationship by electron beam CT. J Comput Assist Tomogr 1998;22:560–568.
160. Lim C, Kim WH, Kim SC, Lee JY, Kim SJ, Kim YM. Truncus arteriosus with coarctation of persistent fifth aortic arch. Ann Thorac Surg 2002;74:1702–1704.
161. Taneja K, Sharma S, Kumar K, Rajani M. Comparison of computed tomography and cineangiography in the demonstration of central pulmonary arteries in cyanotic congenital heart disease. Cardiovasc Intervent Radiol 1996;19:97–100.
162. Choe KO, Hong YK, Kim HJ, et al. The use of high-resolution computed tomography in the evaluation of pulmonary hemodynamics in patients with congenital heart disease: in pulmonary vessels larger than 1 mm in diameter. Pediatr Cardiol 2000;21:202–210.
163. Chen SJ, Wang JK, Li YW, Chiu IS, Su CT, Lue HC. Validation of pulmonary venous obstruction by electron beam computed tomography in children with congenital heart disease. Am J Cardiol 2001;87:589–593.
164. Haramati LB, Glickstein JS, Issenberg HJ, Haramati N, Crooke GA. MR imaging and CT of vascular anomalies and connections in patients with congenital heart disease: significance in surgical planning. Radiographics 2002;22:337–347; discussion 348–349.
165. Kaemmerer H, Stern H, Fratz S, Prokop M, Schwaiger M, Hess J. Imaging in adults with congenital cardiac disease (ACCD). Thorac Cardiovasc Surg 2000;48:328–335.
166. Becker C, Soppa C, Fink U, et al. Spiral CT angiography and 3D reconstruction in patients with aortic coarctation. Eur Radiol 1997;7:1473–1477.
167. Gerber TC, Sheedy PF, Bell MR, et al. Evaluation of the coronary venous system using electron beam computed tomography. Int J Cardiovasc Imaging 2001;17:65–75.
168. Schaffler GJ, Groell R, Peichel KH, Rienmuller R. Imaging the coronary venous drainage system using electron-beam CT. Surg Radiol Anat 2000;22:35–39.
169. Shinbane JS, Girsky MJ, Mao S, Budoff MJ. Thebesian valve imaging with electron beam CT angiography: implications for resynchronization therapy. Pacing Clin Electrophysiol 2004; 27(11):1566–1567.
170. Chugh SS, Blackshear JL, Shen WK, Hammill SC, Gersh BJ. Epidemiology and natural history of atrial fibrillation: clinical implications. J Am Coll Cardiol 2001;37:371–378.
171. Schwartzman D, Kuck KH. Anatomy-guided linear atrial lesions for radiofrequency catheter ablation of atrial fibrillation. Pacing Clin Electrophysiol 1998;21:1959–1978.
172. Yang M, Akbari H, Reddy GP, Higgins CB. Identification of pulmonary vein stenosis after radiofrequency ablation for atrial fibrillation using MRI. J Comput Assist Tomogr 2001;25:34–35.